

Important Descriptors and Descriptor Groups of Curie Temperatures of Rare-earth Transition-metal Binary Alloys

Hieu Chi Dam^{1,2,3}, Viet Cuong Nguyen⁴, Tien Lam Pham^{1,5}, Anh Tuan Nguyen⁶,
Kiyoyuki Terakura^{1,2}, and Takashi Miyake^{2,5,7}, and Hiori Kino^{2,5}

¹*Japan Advanced Institute of Science and Technology, 1-1 Asahidai, Nomi, Ishikawa
923-1292, Japan*

²*CMF², MaDIS, NIMS, Tsukuba, Ibaraki 305-0047, Japan*

³*JST, PRESTO, 4-1-8 Honcho, Kawaguchi, Saitama, 332-0012, Japan*

⁴*HPC Systems Inc., Japan*

⁵*ESICMM, NIMS, Tsukuba 305-0047, Japan*

⁶*Hanoi Metropolitan University, 98 Duong Quang Ham, Cau Giay, Hanoi, Vietnam*

⁷*CD-FMat, AIST, Tsukuba, Ibaraki 305-8568, Japan*

We analyze the Curie temperatures of rare-earth transition metal binary alloys using machine learning. In order to select important descriptors and descriptor groups, we introduce a newly developed subgroup relevance analysis and adopt hierarchical clustering in the representation. We execute exhaustive search and demonstrate that our approach results in the successful selection of important descriptors and descriptor groups. It helps us to choose the combination of descriptors and to understand the meaning of the selected combination of descriptors.

Magnets are now widely used and play an important role in energy savings.^{1,2)} One of the most important applications of magnets is electric motors, whose performance significantly depends on the performance of magnets. Nd-Fe-B based rare-earth magnets are the strongest among the existing permanent magnets, and are almost the only type of permanent magnets that meets the stringent performance requirements of the recent electric motors. However one of the problems with Nd-Fe-B magnets is the relatively low Curie temperature compared to the operation temperatures of the motors. Therefore, many researchers have carried out studies to overcome this drawback, including the exploration of new magnets.

The Curie temperature (T_C) is one of the most important physical quantities of magnets, but unfortunately, it is one of the most difficult physical quantities to predict correctly. There are several theory-driven methods for evaluating the T_C of magnetic materials.³⁾ One

of the basic approaches is to solve an (extended) Hubbard model by using various low-energy solvers. In principle, this method is expected to be accurate. However Anisimov et al. showed that the results are sensitive to the effective parameters and details of the low energy solver.⁴⁻⁶⁾ Therefore, this approach is still at the level of testing the formalism for simple systems like pure transition-metal magnets.

Atomistic spin model is the most common choice for practical application to more complex systems.³⁾ The spin model is constructed from the magnetic moment at each atomic site and the intersite magnetic exchange-couplings based on the assumption of fixed magnitude of spin moments. The parameters are evaluated using the first-principles calculations.³⁾ This method can be applied to rare-earth magnets. Usually, the model is simplified further, and is restricted to the TM-3d and RE-4f spins. Then, T_C s is evaluated, usually in the mean field approximation. The mean field approximation, however, usually overestimates T_C s. Thus, there exist many sources of error in the T_C evaluation using the atomistic spin model. The development of theoretical methods for the estimation of the T_C is still underway.

In contrast to the deductive approaches described so far, there is now a movement toward utilizing inductive approaches, i.e., data-driven methods for estimating T_C , and there have been many reports of successful prediction of the physical quantities using such methods.⁷⁻¹²⁾ The data-driven approach accumulates data, prepares descriptors, makes a model with the descriptors, and finally predicts the values of physical quantities of new materials. One of the key points to be considered for successful prediction is the choice of descriptors. A typical example of descriptor selection can be seen in the work by Ghiringhelli et al., where a regression model is used to predict the energy difference between zinc blende or wurtzite and rocksalt structures.¹³⁾ They used a linear regression model, and first prepared basic descriptors. However, a linear regression model with only the basic descriptors has low description power. Then, they performed various operations on the basic descriptors and produced a number of nonlinear combinations among the basic descriptors. This resulted in an increase in the prediction power. They shrank the number of descriptors using LASSO and finally employed exhaustive search to find the best linear regression model. Their work shows that the combination of descriptors is important for increasing the accuracy of the regression model.

Usually, we select the best regression model and discard all the others (performance-optimized model). However we know that there exist many regression models, where the combination of the descriptors is different from the one that has the best score, but the score of which is as good as the best one indicated by the exhaustive search method. (The best

| Category | Descriptors |
|--|---|
| Atomic properties of transition metals (T) | $Z_T, r_T, r_T^{cv}, IP_T, \chi_T, S_{3d}, L_{3d}, J_{3d}$ |
| Atomic properties of rare-earth metals (R) | $Z_R, r_R, r_R^{cv}, IP_R, \chi_R, S_{4f}, L_{4f}, J_{4f}, g_J, J_{4f}g_J, J_{4f}(1 - g_J)$ |
| Structural information (S) | $C_T, C_R, d_{T-T}, d_{T-R}, d_{R-R}, N_{T-R}, N_{R-R}, N_{R-T}$ |

Table I. Transition metal, rare-earth, and structural descriptors. See also the supporting information.¹⁸⁾

score means, for example, the largest R^2 value in the regression model.) There exists another strategy where we choose the regression model the score of which is not the best, but is high. For example, we can choose low cost descriptors, where "low cost" means easy or literally low cost to evaluate through experiments or calculations. This model is usually referred to an operation-optimized model. Okada et al. devoted considerable effort to the latter problem. They showed the scores of regression models as the density of states to understand the overall structure in one way, and plotted the best scores as a function of the combinations in another way, such as the indicator diagram, to select the best combinations depending on the purpose of the analysis.^{14–16)}

Yet, it is not easy to understand the relationship and structures among descriptors from a huge list of scores and descriptors. Informatics treatment usually ignore the importance of the meaning of the descriptors, though they are physical parameters that physicists regard as important. However we hope that we can extract more information from the huge data. In the present work, we introduce a well-defined subgroup concept to clarify the relationship among descriptors. Our method can also elucidate how to choose combination of descriptors systematically as well as how to understand the meaning of descriptors.

Our target variable is the experimental T_C of the rare-earth transition-metal binary stoichiometry alloys considered in this study.¹⁷⁾ We select the descriptors from the element dependent categories (R for rare-earth elements and T for transition metal elements), and utilize the knowledge of the conventional theory-driven method. The key parameters of the effective theory-driven models are related to the properties of the constituent elements and/or structural parameters. For example, the orbital energy level increases (becomes deeper) as the atomic number Z increases. The electron interaction becomes stronger as the atomic orbital becomes

more localized. The magnetic exchange-couplings are associated with the strength of the electron interaction and transfer integrals. The coupling strength between TM-3d and RE-4f (through RE-5d) is crucial for discussing the RE dependence of magnetism. This strength is proportional to the 3d-4f effective exchange coupling and the 4f total spin projected onto the 4f total angular momentum J_{4f} . The latter quantity is given by $J_{4f}(1 - g_J)$, with g_J being the Landé g-factor. We also add the descriptors from the structure-related category (S) to describe the ratio of the elements as well as the real volume or spatial dependent simple variables to distinguish, e.g., $\text{Th}_2\text{Zn}_{17}$ and $\text{Th}_2\text{Ni}_{17}$ polytypes. We list the descriptors in Table I, and give their detailed explanations in the supporting information.¹⁸⁾

As a regression model, we employ kernel ridge regression with the radial basis function kernel. Kernel ridge regression can include the non-linear effects of the descriptors and has much stronger power to fit the target functions with the descriptors, though there exist a demerit of taking much more time to fit/predict the regression models than the linear regression does. We used Python scripts with `mpi4py`, `scipy` and `scikit-learn`.^{19–21)} Our scores in the regression models are the R^2 values, which we evaluate in the leave-one-out cross validation.

First, we analyze the descriptors. We take Pearson's correlation coefficient between the descriptors. For the T category, the absolute values of Pearson's correlation coefficient among the three descriptors, Z_T , r_T , and S_{3d} , are the same, namely 1, which means that their contributions are the same in the regression model after the normalization procedure. Therefore, the number of independent descriptors is reduced from 27 to 25. Then, we perform exhaustive search for $2^{25} - 1 = 3.3 \times 10^7$ regression models where the combinations of descriptors are different, and evaluate their accuracy values (scores).

Usually, we evaluate the score of the regression model; however, we want to evaluate the importance of the descriptors. Therefore, we change the viewpoint from the regression model to the descriptor in order to discuss the importance of the latter. We use relevance analysis,^{22,23)} which roughly corresponds to the linear response theory with respect to the descriptors. (We explain the scores and relevance analysis in the supporting information.¹⁸⁾) It originally utilizes the change in values when we remove/add a descriptor. The former corresponds to the leave-one-out experiment, while the latter corresponds to the add-one-in experiment. The descriptor is strongly or weakly relevant when its accuracy score changes meaningfully in the leave-one-out or the add-one-in experiment, respectively.

Our first relevance analysis is based on strong relevance. We found that only the descriptor, C_R , is strongly relevant. We can verify the importance of C_R when we plot C_R vs T_C . Almost all the points are placed in the bottom-left side of the right panel of Fig. 1. Thus, it is

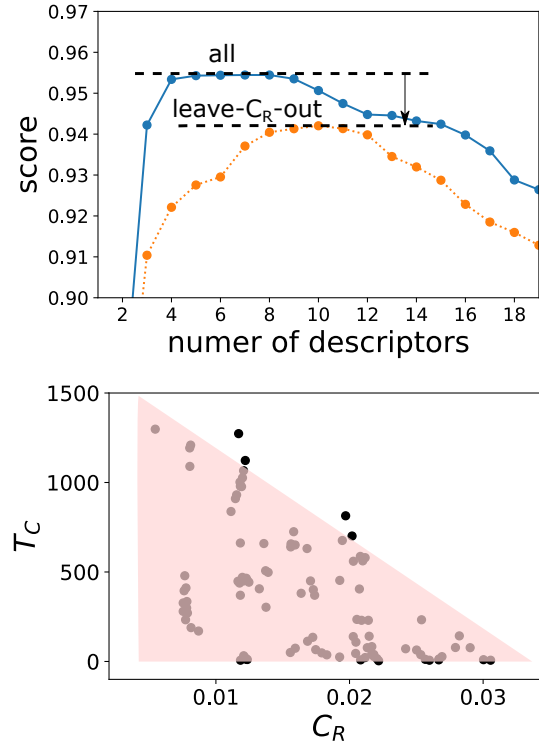


Fig. 1. (Color online) Top panel: The blue line shows the best score for each number of descriptors. The orange dotted line shows the score when C_R is removed. Bottom panel: C_R (\AA^{-3}) vs T_C ($^{\circ}\text{C}$).

clear that C_R has a considerable influence on the T_C . It should be noted that that we will not be able to find such a relationship if we simply execute the regressions.

We notice that relevance analysis can be done not only for a descriptor, but also for a subgroup of descriptors. We define groups and subgroups in this paragraph. The second relevance analysis is based on weak relevance, where, in the original prescription, we add another *descriptor* to the set of descriptors, which we must define. We define the groups and subgroups here, and make use of them in the relevance analysis. We utilize hierarchical clustering analysis, where the distance between descriptors is one minus the absolute values of Pearson's correlation coefficient. We can define the groups or subgroups of descriptors that are clustered based on the criteria of them being within distance, d , of each other. For example, we can define four groups at $d = 0.5$. Two of them have the same descriptors as those of the T and R categories, while the other two have that of the original S category. (We call the original cluster as *category* and the cluster by the hierarchical analysis as *group*.) The d_{TR} constitutes a group, while the other S category descriptors constitute the other. It is not surprising that the grouping at $d = 0.5$ is almost the same as the categories defined a priori

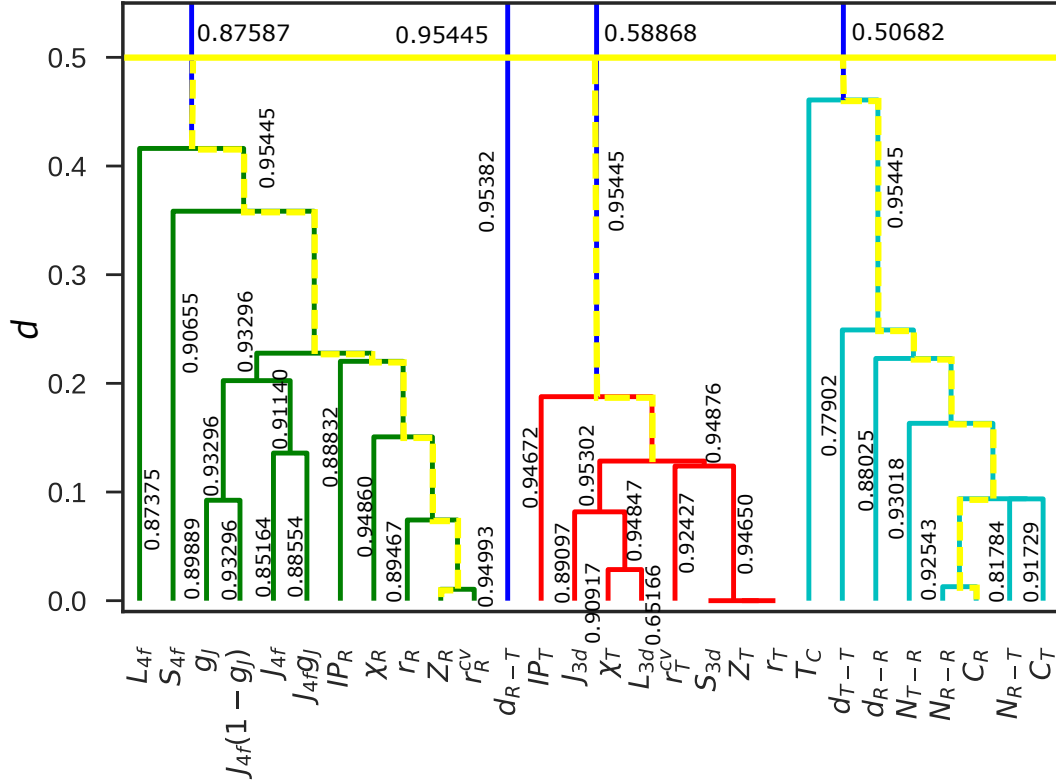


Fig. 2. (Color online) R^2 scores of the subgroup relevance analysis on the hierarchical clustering of the descriptors. We include T_C in the dendrogram. The group R (green) is from L_{4f} to r_R^{cv} . The group T (red) is from IP_T to r_T . The group S (cyan) is from d_{TT} to C_T . The group d_{TR} is made of the descriptor d_{TR} . The horizontal values are strong relevance values and the tilted values are weak relevance values. The vertical axis shows the distance, d , and the values are one minus the absolute values of Pearson's correlation coefficient. The paths of the highest value (0.95445) are colored in yellow dashed lines. See details in the main body also.

as T, R, and S when we remember the definition of the descriptors of the materials. Here, we successfully defined the groups and subgroups, where the groups are almost the same as the original category but are clustered from the data themselves. (We redefine the group S as a result of this clustering. The group S that does not include d_{TR} is different from the category S.)

We can make further advances in this grouping. We notice that the definition of the value of d is unnecessary, but we only have to define the vertical line of the decomposition tree to define the subgroups because the child nodes below the vertical line is the same. (See also Fig. 2. The vertical axis corresponds to d .) Thus, we are able to define many subgroups of the descriptors as sets of the child nodes of the *dendrogram*.

We apply the relevance analysis not to a descriptor but to a subgroup/group. We call this

Table II. The best R^2 score and descriptors as a function of the number of descriptors n .

| n | score | descriptor(s) |
|---|----------|---|
| 2 | 0.8701 5 | C_R, Z_T |
| 3 | 0.9422 2 | C_R, Z_R, Z_T |
| 4 | 0.9533 9 | J_{3d}, C_R, Z_R, Z_T |
| 5 | 0.9542 9 | $L_{3d}, J_{3d}, C_R, Z_R, Z_T$ |
| 6 | 0.9543 9 | $L_{3d}, J_{3d}, \chi_T, C_R, Z_R, Z_T$ |
| 7 | 0.9544 5 | $L_{3d}, J_{3d}, \chi_T, C_R, Z_R, Z_T, r_T^{cv}$ |
| 8 | 0.9544 5 | $L_{3d}, J_{3d}, \chi_T, IP_T, C_R, Z_R, Z_T, r_T^{cv}$ |

method *subgroup relevance analysis*. We plotted the result in Fig. 2. The horizontal score is evaluated in the leave-one-out experiment and is related to the strong relevance, while the vertical scores are evaluated in the add-one-in experiment and is related to the weak relevance. Note that the score of a subgroup belonging to a group is evaluated under the condition that we must use at least one descriptor in the subgroup, and any descriptors belonging to the other groups can be added in the weak relevance analysis.

In Fig. 2, the weak relevance values, or add-one-in values, are written as vertical values. The subgroup containing only r_R has the score, 0.89467, which is the highest score in the condition that we must take the subgroup r_R in the group R and we can take any descriptors in the other groups. (A subgroup which has a descriptor is also a subgroup.) The subgroup containing r_R , Z_R , and r_R^{cv} has the score, 0.95445, which is the highest score in the condition that we must take at least one descriptor in the subgroup r_R , Z_R , and r_R^{cv} of the group R and we can take any descriptors in the other groups as explained in the previous paragraph.

The sole descriptor Z_R in the group R has the highest score (0.95445). It means that Z_R can solely represent the group R. This is also the case for the C_R subgroup in the group S. However the structure of the group T is different from those of the groups R and S. The subgroup made of J_{3d} , χ_T , r_T^{cv} , Z_T (and r_T and S_{3d}) has the highest score (0.94876), but its child subgroup descriptors have smaller scores (0.92427 and 0.94650). It means that there exists no single descriptor that can represent the overall nature of the group T. When we examine all the combinations made of J_{3d} , χ_T , r_T^{cv} , Z_T , we find that Z_T takes the best score (0.95450) if we choose only one of the descriptors among them, a set of Z_T and J_{3d} is the best (0.95339) for two descriptors, and a set of Z_T , J_{3d} and L_{3d} is the best (0.95445) for three descriptors. We note that the descriptor Z_T has the same effect as S_{3d} . We discuss interpretation of the result later.

We can also obtain the importance of the groups from the horizontal values above the yellow solid line in Fig. 2. They are the strong relevance values, or leave-one-out values of the groups T, R, and S. For example, the group R has the value, 0.87587, which is the best score when we remove all the descriptors of the group R. The better the score is, the less important the group is. The value, 0.50682, is the smallest among them, which means that the group S is the most important among the groups. On the other hand, the least important group is R, the value of which is 0.87587. It means that the score still holds a high value even if we exclude all the descriptors in the group R. Therefore, the importance of group R is the lowest among T, S, and R.

We have added additional explanation in Fig. 2. The descriptor $J_{4f}(1 - g_J)$ can represent the subgroup containing $g_J, \dots, J_{4f}g_J$, but the score is 0.93296, which is lower than the score 0.95445 of Z_R . We have also added a comment on the group of d_{TR} . The strong relevance value is 0.95445 and the weak relevance value is 0.95382. The facts that their difference is small and that the weak relevance value is smaller than the strong relevance value mean that the existence of the group d_{TR} makes the regression model worse.

Here, we compare the result of the subgroup relevance analysis shown in Fig. 2 with the best score having n descriptors without the subgroup relevance analysis, which is shown in table II. The set of C_R , Z_R , and Z_T has the best score (0.94222) for $n = 3$. The set of C_R , Z_R , Z_T , and J_R has the best score (0.95339) for $n = 4$. The set of C_R , Z_R , Z_T , J_R , and L_{3d} has the best score (0.95429) for $n = 5$. The descriptor sets are made of the most important descriptors in group R (Z_R), group S (C_R), and group T (Z_T when we choose a descriptor; J_{3d} and Z_T when we choose two descriptors; and J_{3d} , L_{3d} , and Z_T when we choose three descriptors.) These combinations are the same as the analysis in the previous paragraph. Thus, the subgroup relevance analysis successfully illustrates the structure among the descriptors and their importance.

One may think that the difference in the scores are quite tiny. For example, 99.0% value of the global best score is 0.944, which roughly corresponds to the best score with 12 descriptors (see also Table I in the supporting information).¹⁸⁾ However the predicting ability changes drastically. We plot the "RMSE" between the best models with n descriptors in Fig. 2 in the supporting information.¹⁸⁾ It can be clearly seen that the prediction abilities for $n=3$ to 8 is qualitatively different from those for $n \geq 9$, but the difference of the score of the best model with 9 (10) descriptors to the global best model is only 0.1% (0.4%). The difference in the score looks tiny at a glance, but is meaningful in this data and regression model. (One must also discuss the total density of state of the scores to discuss the meaningful difference of the

scores, but it is beyond the scope of this study.^{14–16)}

The ordering of the scores of the models (combinations of descriptors) can be changed according to the details of the regression scheme and noise in the data, because the differences in the scores are quite small (Table II in the main body and Table I in the supporting information).¹⁸⁾ Thus, just showing the best models with n descriptors may give us wrong information. However the relevance analysis can give us more significant differences. The dendrogram, or grouping, does not depend on the scores of the models because it is made only of the distances between the descriptors. Even if there exists noise in the data, which may affect the scores of the model, we can expect that similar descriptors will give similar scores. The subgroup relevance analysis can illustrate how the distances, or the similarities, between the descriptors affect to the models.

Here, we further explain the advantage of the expression with the dendrogram. For example, we can easily choose r_R^{cv} if we do not want to use Z_R if the importance is expressed as in Fig. 2. It enables us to find the next best route, that is, to go upward and try a new branch downward in the tree structure. We believe that this expression is much better than simply providing a list, and it is much easier to find out the operation-optimized regression models.

We can conclude that the descriptor C_R is strongly relevant when we define the subgroups at $d \sim 0$ and execute the leave-one-out experiment. The original relevance analysis is the special case of the subgroup relevance analysis. Therefore, the subgroup relevance analysis is a natural extension of the original relevance analysis.

Here, we note the possible interpretation of the regression model in the context of condensed matter physics, where we know that physics should depend not on J_4f but on $J_4f(1 - g_J)$ in the effective model Hamiltonian. We, however, found more important descriptors, e.g., Z_R and r_R^{cv} in the group R and J_{3d} in the group T. It is more plausible that the regression model found a relationship similar to the generalized Slater-Pauling curve for Curie temperature as a function of C_R and Z_T and Z_R , and that the other effects are only marginal.²⁴⁾ We introduced many descriptors that cannot appear in the atomic-scale effective model Hamiltonian, and the regression model simply selected the *inter-scale* regression model including the macro scale parameter C_R first and Z_T and Z_R next, which do not directly appear in the effective model Hamiltonian because their relationships are more apparent. It should be noted that the number of data, only about a hundred, is too few to discuss the details because it can easily change the prediction accuracy as discussed in the supporting information.¹⁸⁾

We cannot avoid errors in T_{CS} because of experimental errors and human errors. The latter is mainly because AtomWork does not allow web scraping. We examine the possibil-

ity of outlier detection using machine learning. We show a plot of experimental T_C s versus predicted ones in the supporting information.¹⁸⁾ The overall coincidence is good from 0K to ~ 1300 K, but there exist a few outliers. We mainly check the outliers of T_C s and fix the errors again and again if there are any. We found three major errors and a minor error. After fixing these errors, we evaluated the cross-validation test scores again for the best n descriptors of the original regression model. The best R^2 was 0.96688. By using machine learning, it may be able possible to find data errors efficiently; however, it cannot detect data prediction of which appears consistent with the experimental values accidentally.

We employed Pearson's correlation coefficient to define the distance in this study. However, there exist many choices for the distance. It depends on the problem whose representation is the most appropriate in the unsupervised learning part. We use the similarity, or distance, between materials to find the regression model, but usually discard the similarity between descriptors to make the regression model. We, however, utilized the latter similarity, and therefore took full advantage of the similarity of the data in this prescription.

We showed that the distances between the descriptors are useful to illustrate the importance of descriptors and descriptor groups. This result is not strange when the descriptors have some physical meaning. There exists, however, minor discrepancies in the subgroup containing Z_R , J_{3d} , and L_{3d} in the dendrogram. This is a limitation of this theory; however, it is possible to overcome this difficulty. We used the distance between the descriptors to explain the scores of the relevance analysis, but its inverse problem is also possible. We can set the value of distances between the descriptors, or the structures of the dendrogram, to be more consistent with the scores of the relevance analysis.

We can consider many variants of the subgroup relevance analysis. We took the best *descriptor* from the subgroup shown in yellow in Fig. 2. Thus, we were able to show the best descriptors in the subgroup. Another method is to take the best *subgroup* in the downstream to a specified subgroup. Then, we will be able to understand the relationship among subgroups, and we can easily change them depending on the purpose.

Note that the Monte-Carlo tree search also utilizes the same nature of tree structures. There may be a route to find out the almost best regression model by utilizing subgroup decomposition without performing expensive exhaustive search.

In summary, we studied the data-driven approach on the Curie temperature of rare-earth transition metal stoichiometric alloys. We successfully made regression models that achieved high scores from our descriptors. We developed subgroup relevance analysis and successfully illustrated the importance, relationship, and structures among the descriptors from a huge list

of exhaustive search. In addition, it should be noted that our method makes full use of the similarity of the given data.

Acknowledgments

This work was partly supported by PRESTO and by the “Materials Research by Information Integration” Initiative (MI²I) project of the Support Program for Starting Up Innovation Hub, both from the Japan Science and Technology Agency (JST), Japan; by the Elements Strategy Initiative Project under the auspices of MEXT; and also by MEXT as a social and scientific priority issue (Creation of New Functional Devices and High-Performance Materials to Support Next-Generation Industries; CDMSI) to be tackled by using a post-K computer. The calculations were partly carried out on Numerical Materials Simulator at NIMS.

References

- 1) S. Sugimoto, J. Phys. D: Appl. Phys. **44**, 064001 (2011).
- 2) Satoshi Hirosawa, Masamichi Nishino, and Seiji Miyashita, Adv. Nat. Sci: Nanosci. Nanotechnol. **8** 013002 (2017).
- 3) Takashi Miyake and Hisazumi Akai, J. Phys. Soc. Jpn. **87**, 041009 (2018), and references therein.
- 4) A. S. Belozerov, I. Leonov, and V. I. Anisimov, Phys. Rev. B **87** 125138 (2013).
- 5) A S Belozerov and V I Anisimov, Journal of Physics: Condensed Matter **26** 375601 (2014)
- 6) A. A. Katanin, A. S. Belozerov, and V. I. Anisimov, Phys. Rev. B **94** 161117 (2016).
- 7) Radislav Potyrailo, Krishna Rajan, Klaus Stoewe, Ichiro Takeuchi, Bret Chisholm and Hubert Lam, ACS Comb. Sci., **13**, 579 (2011).
- 8) Krishna Rajan, Informatics for Materials Science and Engineering: Data-driven Discovery for Accelerated Experimentation and Application, Butterworth-Heinemann (2013).
- 9) Ankit Agrawal and Alok Choudhary, APL Materials, **4**, 053208 (2016).
- 10) Anubhav Jain, Geoffroy Hautier, Shyue Ping Ong, Kristin Persson, J. Mater. Res., **31**, 977 (2016).
- 11) Yue Liu, Tianlu Zhao, Wangwei Ju, Siqi Shi, J Materiomics **3**, 159 (2017).
- 12) Wencong Lu, Ruijuan Xiao, Jiong Yang, Hong Li, Wenqing Zhang, J Materiomics **3**, 191 (2017).
- 13) Luca M. Ghiringhelli, Jan Vybiral, Sergey V. Levchenko, Claudia Drax and Matthias Scheffler, Phys. Rev. Lett. **114**, 105503 (2015).
- 14) Kenji Nagata, Jun Kitazono, Shin-ichi Nakajima, Satoshi Eifuku, Ryoï Tamura and Masato Okada, IPSJ Transactions on Mathematical Modeling and Its Applications, **8**, 23 (2015).
- 15) Tatsu Kuwatani, Kenji Nagata, Masato Okada, Takahiro Watanabe, Yasumasa Ogawa, Takeshi Komai and Noriyoshi Tsuchiya, Scientific Reports **4**, 7077 (2014).
- 16) Hiroko Ichikawa, Jun Kitazono, Kenji Nagata, Akira Manda, Keiichi Shimamura, Ryōichi Sakuta, Masato Okada, Masami K. Yamaguchi, So Kanazawa, Ryusuke Kakigi, Front. Hum. Neurosci. **8** 480 (2014).

- 17) The values of experimental T_C are taken from the AtomWork database, <http://crystdb.nims.go.jp/>.
- 18) (Supplemental material) More detailed explanations are available online.
- 19) Fabian Pedregosa, Gael Varoquaux, Alexandre Gramfort, Vincent Michel, Bertrand Thirion, Olivier Grisel, Mathieu Blondel, Peter Prettenhofer, Ron Weiss, Vincent Dubourg, Jake Vanderplas, Alexandre Passos, David Cournapeau, Matthieu Brucher, Matthieu Perrot, Edouard Duchesnay, *Journal of Machine Learning Research* **12**, 2825, (2011).
- 20) Travis E. Oliphant, *Computing in Science & Engineering*, **9**, 10 (2007).
- 21) K. Jarrod Millman and Michael Aivazis, *Computing in Science & Engineering*, **13**, 9 (2011),
- 22) Lei Yu, Huan Liu, *J. Mach. Learn. Res.* **5**, 1205 (2004).
- 23) S. Visalakshi and V. Radha, in *2014 IEEE International Conference on Computational Intelligence and Computing Research* (2014), pp. 1-6.
- 24) For example, C Takahashi, M Ogura and H Akai, *Journal of Physics: Condensed Matter*, **19**, 365233 (2007).

Important Descriptors and Descriptor Groups of Curie Temperatures of Rare-earth Transition-metal Binary Alloys: Supporting Information

1 Descriptors

We collected the experimental data of 101 binary compounds consisting of transition metals and rare-earth metals from the Atomwork database of NIMS [1], including the crystal structure of the compounds and their observed T_C . To represent the structural and physical properties of each binary compound, we use a combination of 28 descriptors. We divide all 28 descriptors into three categories.

The first category pertains to the descriptors describing the atomic properties of the transition-metal constituent, including the (1) atomic number (Z_T), (2) atomic radius (r_T), (3) covalent radius (r_T^{cv}), (4) ionization potential (IP_T), (5) electronegativity (χ_T), (6) spin angular momentum (S_{3d}), (7) orbital angular momentum (L_{3d}), and (8) total angular momentum (J_{3d}) of the 3d electrons. The selection of these descriptors originates from the physical consideration that the intrinsic electronic and magnetic properties will determine the 3d orbital splitting at transition-metal sites.

In the same manner, we design the second category pertaining to the descriptors for describing the properties of the rare-earth metal constituent, including the (9) atomic number (Z_R), (10) atomic radius (r_R), (11) covalent radius (r_R^{cv}), (12) ionization potential (IP_R), (13) electronegativity (χ_R), (14) spin angular momentum (S_{4f}), (15) orbital angular momentum (L_{4f}), and (16) total angular momentum (J_{4f}) of the 4f electrons. To capture the effect of the 4f electrons better, we add three additional descriptors for describing the properties of the constituent rare-earth metal ions, including (17) the Landé factor (g_J), (18) the projection of the total magnetic moment onto the total angular momentum ($J_{4f}g_J$), and (19) the projection of the spin magnetic moment onto the total angular momentum ($J_{4f}(1 - g_J)$) of the 4f electrons. The selection of these descriptors originates from the physical consideration that the magnitude of the magnetic moment will determine T_C .

It has been well established that information related to the crystal structure is very valuable in relation to understanding the physics of binary compounds with transition metals and rare-earth metals. Therefore, we design the third category with structural descriptors that roughly represent the structural information at the transition metal and rare-earth metal sites, which are (20) the concentration of the transition metal (C_T), (21) the concentration of the rare-earth metal (C_R), (22) the average distance between a transition-metal site and the nearest transition-metal site (d_{T-T}), (23) the average distance between a transition-metal site and the nearest rare-earth-metal site (d_{T-R}), (24) the average distance between a rare-earth metal-site and the nearest rare-earth-metal site (d_{R-R}), (25) the average number of rare-earth-metal sites surrounding a transition-metal site within the distance less than 5.0 Å (N_{T-R}), (26) the average number of rare-earth-metal sites surrounding a rare-earth-metal site within the distance less

than 10.0 Å(N_{R-R}), and (27) the average number of transition-metal sites surrounding a rare-earth-metal site within the distance less than 5.0 Å(N_{R-T}). The values of these descriptors are calculated from the crystal structures of the compounds from the literature.

2 Strong Relevance and Weak Relevance

We define the prediction ability $PA(\mathbf{S})$ of descriptors by the maximum prediction accuracy that the model can achieve by using the descriptors in a subset \mathbf{s} of a set \mathbf{S} of descriptors as follows:

$$PA(\mathbf{S}) = \max_{\forall \mathbf{s} \subset \mathbf{S}} R_s^2, \quad (1)$$

where R_s^2 is the value of the coefficient of determination R^2 achieved by the model using a descriptor set \mathbf{s} . ($R^2 = 1 - \frac{\sum_i (y_i - y_i^{pred.})^2}{\sum_i (y_i - \bar{y})^2}$, where y_i , $y_i^{pred.}$, and \bar{y} are the target value, the predicted value, and the mean target value, respectively.) On the basis of Eq. (1), we can evaluate the relevance [2, 3] of a descriptor for the prediction of T_C by using the expected reduction in the prediction ability caused by removing this descriptor from the full set of descriptors. Let \mathbf{D} be a full set of descriptors, d_i a descriptor, and $\mathbf{D}_i = \mathbf{D} - \{d_i\}$ the full set of descriptors after removing the descriptor d_i . The degree of relevance of the descriptors can be formalized as follows:

Strong relevance: a descriptor is strongly relevant if and only if

$$PA(\mathbf{D}) - PA(\mathbf{D}_i) = \max_{\forall \mathbf{s} \subset \mathbf{D}} R_s^2 - \max_{\forall \mathbf{s} \subset \mathbf{D}_i} R_s^2 > 0. \quad (2)$$

Among the strongly relevant descriptors, a descriptor that causes a larger reduction in the prediction ability when it is removed can be considered as a strong one. The degree of relevance of a strongly relevant descriptor can be computationally estimated by using the **leave-one-out** approach, i.e., by leaving out a descriptor in the currently considered descriptor set and testing how much the prediction accuracy is impaired.

Weak relevance: a descriptor is weakly relevant if and only if

$$PA(\mathbf{D}) - PA(\mathbf{D}_i) = \max_{\forall \mathbf{s} \subset \mathbf{D}} R_s^2 - \max_{\forall \mathbf{s} \subset \mathbf{D}_i} R_s^2 = 0 \text{ and} \\ \exists \mathbf{D}'_i \subset \mathbf{D}_i \text{ such that } PA(\{d_i, \mathbf{D}'_i\}) - PA(\mathbf{D}'_i) > 0. \quad (3)$$

It is clearly seen from Eq. (3) that estimation of the degree of relevance for the weakly relevant descriptors cannot be carried out in a straightforward manner as for the case of the strongly relevant descriptors. Weakly relevant descriptors are descriptors that are relevant for prediction, but they can be substituted by the other descriptors. We can only estimate the degree of relevance for this type of descriptor in specified contexts. For example, in terms of the prediction of T_C , the relevance of a descriptor for an atomic property of transition metal can be examined in the context that all of the descriptors for the atomic properties of rare-earth metals are included in the descriptor set. We define the following additional rule for comparing two weakly relevant descriptors:

Comparison between weakly relevant descriptors: A weakly relevant descriptor d_i is said to be more relevant than the descriptor d_j in the context of having a set of descriptors $\mathbf{M}(d_i, d_j \notin \mathbf{M})$ **if and only if**

$$PA(\{d_i, \mathbf{M}\}) > PA(\{d_j, \mathbf{M}\}). \quad (4)$$

Table 1: The number of descriptors vs the best R^2 score and descriptors.

| n | score | descriptor(s) |
|----|---------|--|
| 1 | 0.32518 | N_{R-T} |
| 2 | 0.87015 | C_R, Z_T |
| 3 | 0.94222 | C_R, Z_R, Z_T |
| 4 | 0.95339 | J_{3d}, C_R, Z_R, Z_T |
| 5 | 0.95429 | $L_{3d}, J_{3d}, C_R, Z_R, Z_T$ |
| 6 | 0.95439 | $L_{3d}, J_{3d}, \chi_T, C_R, Z_R, Z_T$ |
| 7 | 0.95445 | $L_{3d}, J_{3d}, \chi_T, C_R, Z_R, Z_T, r_T^{cv}$ |
| 8 | 0.95445 | $L_{3d}, J_{3d}, \chi_T, IP_T, C_R, Z_R, Z_T, r_T^{cv}$ |
| 9 | 0.95351 | $d_{R-T}, L_{3d}, J_{3d}, \chi_T, IP_T, r_R^{cv}, C_R, N_{R-R}, J_{4f}g_J$ |
| 10 | 0.95065 | $d_{R-T}, L_{3d}, J_{3d}, \chi_T, IP_T, r_R^{cv}, C_R, N_{R-R}, J_{4f}g_J, Z_T$ |
| 11 | 0.94749 | $d_{R-T}, L_{3d}, J_{3d}, \chi_T, IP_T, C_R, N_{R-R}, Z_R, J_{4f}g_J, Z_T, r_T^{cv}$ |
| 12 | 0.94479 | $d_{R-T}, L_{3d}, J_{3d}, \chi_T, IP_T, r_R^{cv}, C_R, C_T, N_{R-R}, Z_R, J_{4f}g_J, r_T^{cv}$ |
| 13 | 0.94456 | $L_{3d}, J_{3d}, \chi_T, J_{4f}, IP_T, C_R, C_T, N_{R-R}, Z_R, Z_T, N_{R-T}, r_T^{cv}, L_{4f}$ |
| 14 | 0.94322 | $d_{R-T}, J_{4f}(1-g_J), L_{3d}, J_{3d}, \chi_T, J_{4f}, IP_R, IP_T, C_R, C_T, N_{R-R}, Z_R, Z_T, N_{R-T}$ |
| 15 | 0.94245 | $d_{R-T}, r_R, J_{4f}(1-g_J), L_{3d}, J_{3d}, \chi_T, IP_T, r_R^{cv}, C_R, C_T, N_{R-R}, Z_T, N_{R-T}, r_T^{cv}, L_{4f}$ |
| 16 | 0.93979 | $d_{R-T}, d_{T-T}, J_{4f}(1-g_J), L_{3d}, J_{3d}, \chi_T, J_{4f}, IP_R, IP_T, C_R, C_T, N_{R-R}, Z_R, Z_T, N_{R-T}, r_T^{cv}$ |
| 17 | 0.93591 | $d_{R-T}, r_R, d_{T-T}, J_{4f}(1-g_J), L_{3d}, J_{3d}, \chi_T, J_{4f}, IP_R, IP_T, r_R^{cv}, C_R, C_T, N_{R-R}, Z_T, N_{R-T}, r_T^{cv}$ |
| 18 | 0.92879 | $d_{R-T}, r_R, d_{T-T}, J_{4f}(1-g_J), L_{3d}, J_{3d}, \chi_T, IP_T, C_R, C_T, d_{R-R}, \chi_R, N_{R-R}, Z_R, Z_T, r_T^{cv}, S_{4f}, N_{T-R}$ |
| 19 | 0.92642 | $d_{R-T}, r_R, d_{T-T}, J_{4f}(1-g_J), L_{3d}, J_{3d}, g_J, \chi_T, IP_T, r_R^{cv}, C_R, C_T, d_{R-R}, \chi_R, N_{R-R}, Z_R, Z_T, r_T^{cv}, N_{T-R}$ |

A comparison of two weakly relevant descriptors can be computationally carried out by using the **add-one-in** approach, i.e., by exclusively adding the two descriptors to the currently considered descriptor set and testing how much the prediction accuracy is improved.

3 Best R^2 Scores and Descriptors

We present a list of the best R^2 scores and descriptors in Table 1. It may appear that the difference in the scores is very small. We originally used ten times ten-fold cross validation (10×10 CV). [4] The best scores of the 10×10 CV are the same for the two digits, i.e., they are 0.95X and 0.960 for $n = 5$ to 10, where X varies. Consequently, the plot of the scores versus n shows a plateau. We recognize that there exist non-negligible statistical errors which affects the relevance analysis. Next, we employ the leave-one-out cross validation because there exist no statistical errors and because we can obtain the most accurate scores from the data. Then, the best scores are the same for the three digits, i.e., they are 0.954X for $n=5$ to 8 in the leave-one-out cross validation, where there is a plateau in the score plot versus n . The difference between the scores becomes 10 times smaller in the latter.

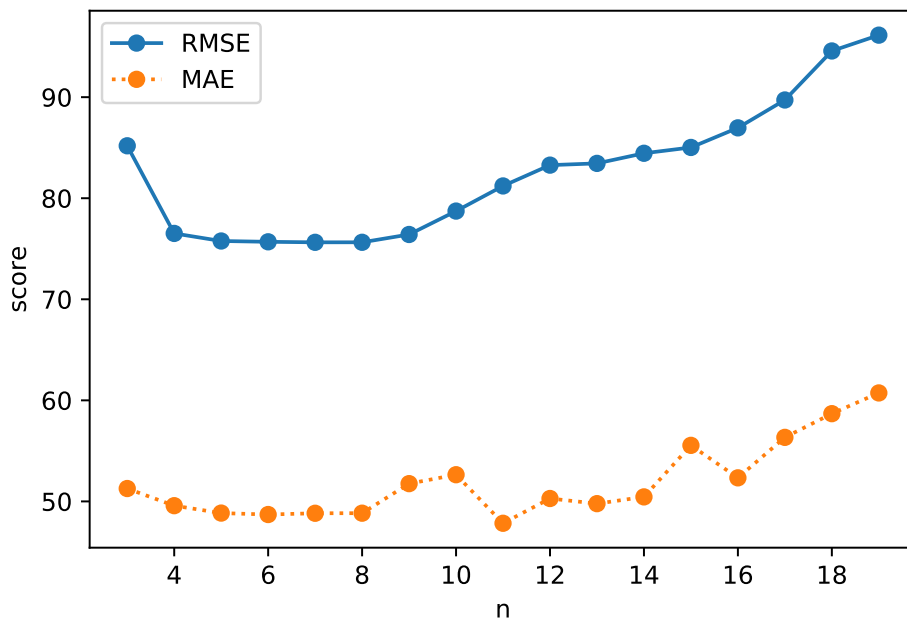


Figure 1: The best RMSE and MAE as functions of the number of descriptors ($^{\circ}\text{C}$).

4 Prediction among the Best n Models

We show the best scores of RMSE and MAE as a function of the number of descriptors (n) in the models in Fig. 1. The score changes gradually as a function of n . One may expect that their predictions are almost the same. We also evaluate the "RMSE" between the leave-one-out cross validated test predictions of the best models with the n descriptors in Fig. 2. We can see that the predictions are almost the same for $n=4$ to 8; however, the deviations are larger in the other cases. Only the best models for $n=4$ to 8 give almost the same predictions. We can also see this trend from the kernel parameters. Note that these figures are the results before fixing the errors in the data.

5 Prediction among the Best n Models after Fixing Errors

We show the scores for RMSE, MAE, and R^2 for the models in Table 1 in Figs. 3 and 4. The models for $4 \leq n \leq 8$ have high scores.

6 Experimental T_C versus CV-predicted T_C

We plot the experimental T_C versus the CV-predicted T_C before and after fixing the errors in Fig. 5 and 6. They show the mean and standard deviation of the predictions. The standard deviations are shown as bars, but almost all of them are smaller than the sizes of the symbols.

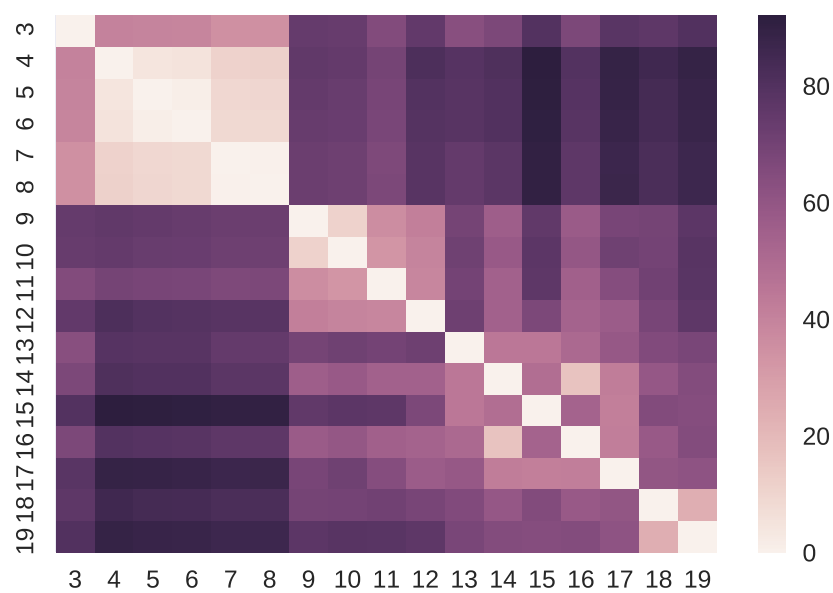


Figure 2: Heatmap of "RMSE" between the best models with n descriptors.

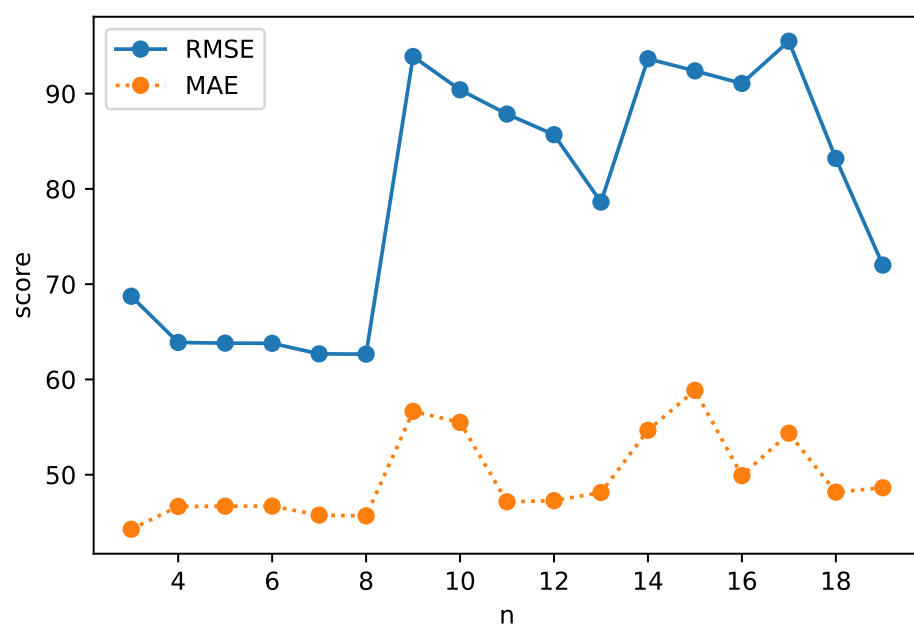


Figure 3: The best RMSE and MAE as functions of the number of descriptors ($^{\circ}$ C).

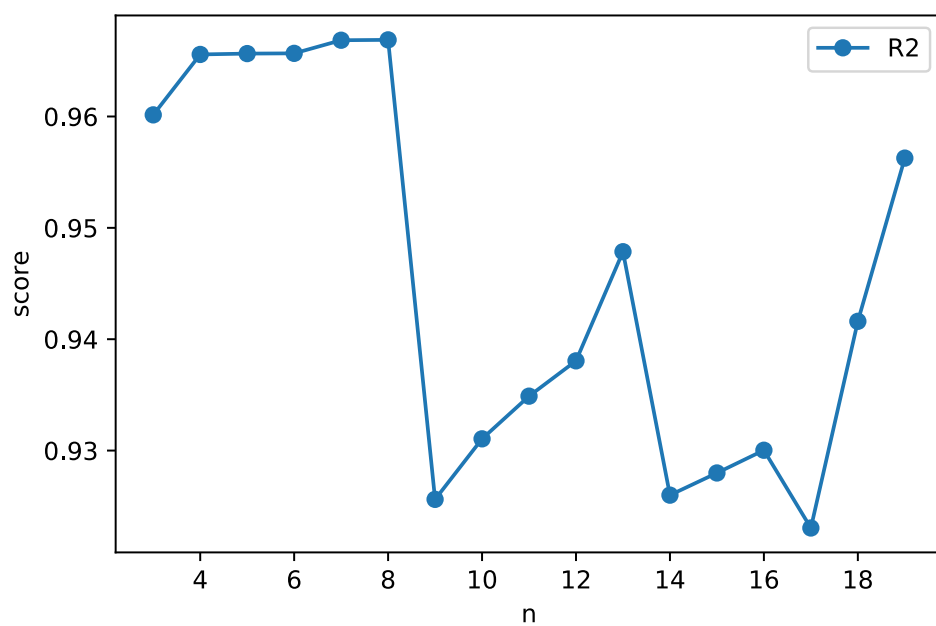


Figure 4: The best R^2 as a function of the number of descriptors.

The overall coincidence is good from 0K to approximately 1300K, but we find a few outliers in Fig. 5. For example, the experimental T_{CS} of SmCo_5 and PrNi_5 are much higher than the predicted ones, whereas the experimental T_{CS} are much smaller for NdCo_5 and NdNi_5 . We find three major errors and a minor error in the experimental T_{CS} including those for SmCo_5 and PrNi_5 .

A new plot obtained after fixing the errors is shown in Fig.6. The predicted values of NdCo_5 and NdNi_5 now are almost the same as the experimental values. We find other outliers, such as the data for Ce_2Co_7 and RCO_5 . However, it appears that these are not because of the errors in the data.

7 Predicted T_{CS} for (RE) Fe_{12}

We examine the prediction ability of the best regression model. We apply the best regression model to (RE) Fe_{12} , which was recently synthesized and attracts much attention. The existing experimental T_{CS} are 508K for NdFe_{12} , [5] 586K for SmFe_{12} , [6] and 483K for YFe_{12} . [7]. On the other hand, the corresponding predicted T_{CS} are 490(19)K, 581(15)K, and 396(10)K, where the crystal structures are obtained from the first-principles calculation and we substituted the Z and quantum-number-related descriptors of La for those of Y.[8] The coincidences of the values of NdFe_{12} and SmFe_{12} are fairly good considering the fact that we do not have the structure data in the training set. The predicted values for DyFe_{12} and GdFe_{12} are 470(11)K and 600(13)K, respectively. However, these predicted values decrease by 120–180K after fixing the errors in the data. The predicted values depend on the value of the L2 penalty term. We add this information as reference.

8 List of Descriptors

We list the original descriptors and T_{CS} before fixing the errors in Tables 2-10. We list the final descriptors and T_{CS} after fixing the errors in Tables 11-19. The number of original materials was 101, but we found a non-stoichiometry material, which was deleted.

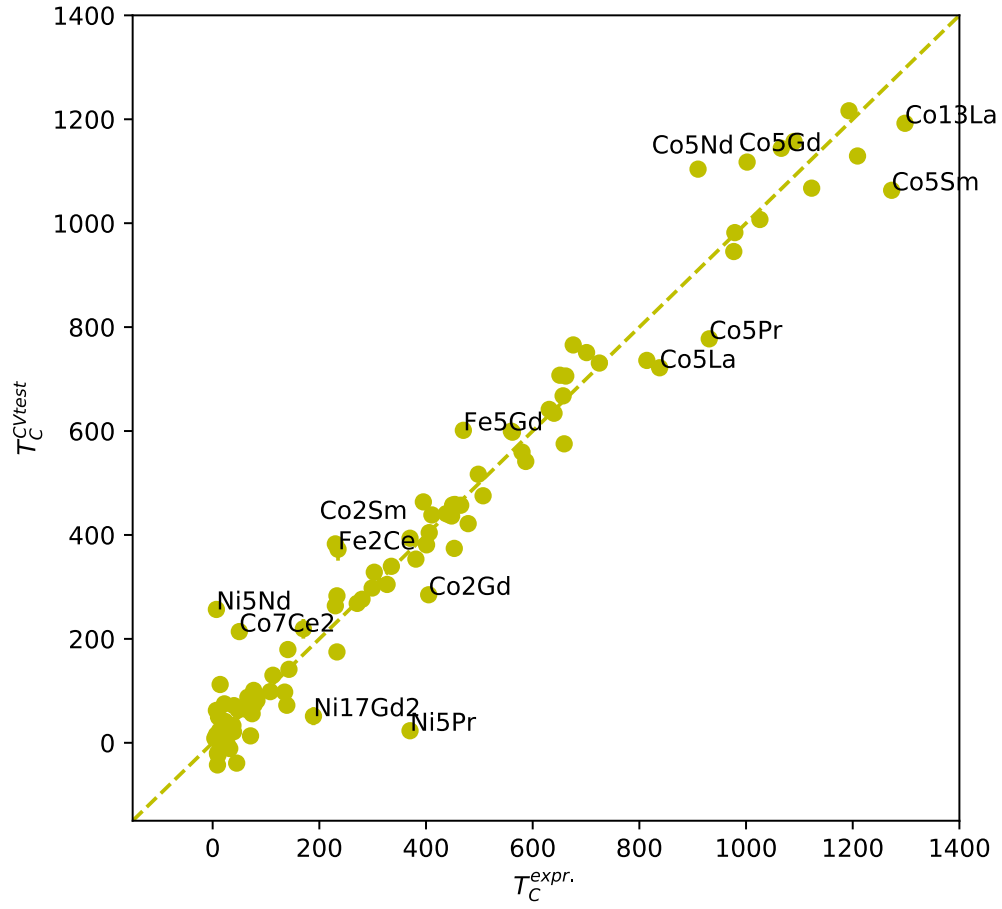


Figure 5: Experimental T_C versus CV-predicted T_C before fixing the errors.

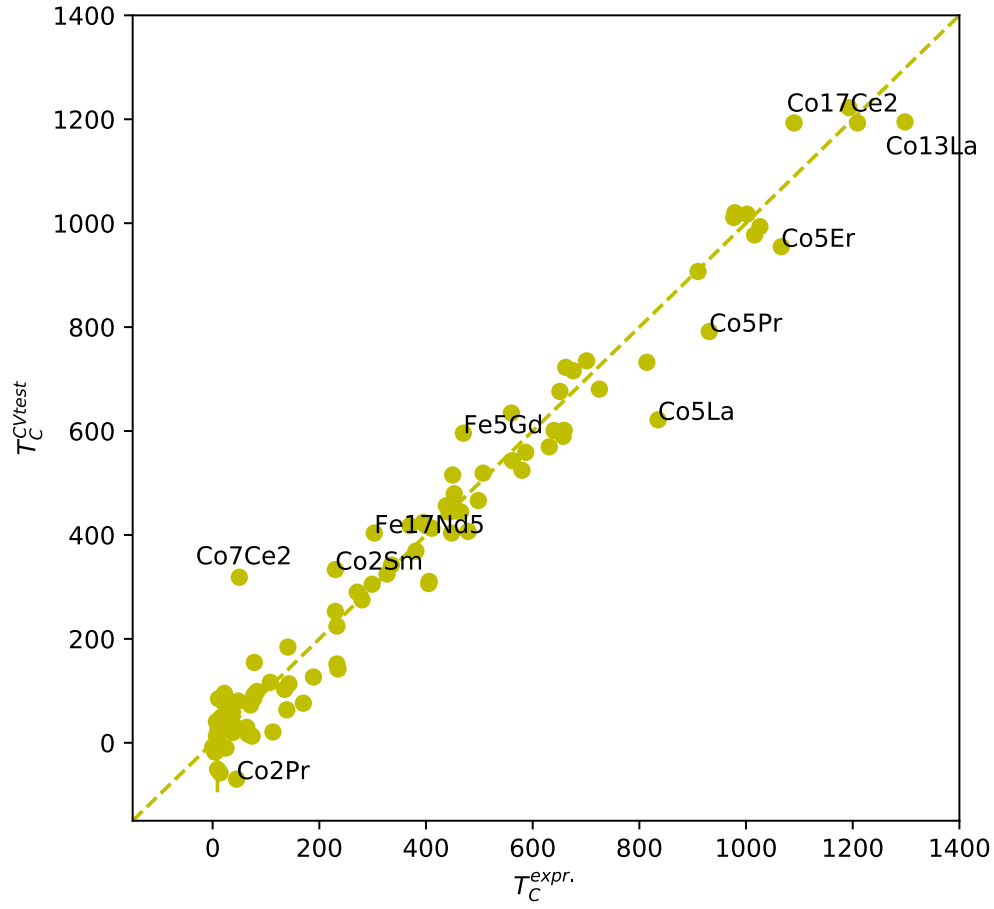


Figure 6: Experimental T_C versus CV-predicted T_C after fixing the errors.

| material | T_C | Z_R | r_R | r_R^{cov} | IP_R | χ_R | S_{4f} | L_{4f} | J_{4f} |
|---------------------|-------|-------|-------|-------------|--------|----------|----------|----------|----------|
| Co17Ce2(Zn17Th2) | 1090 | 58 | 181 | 204 | 534.4 | 1.12 | 0.5 | 3 | 2.5 |
| Co5Ce(CaCu5) | 662 | 58 | 181 | 204 | 534.4 | 1.12 | 0.5 | 3 | 2.5 |
| Co7Ce2(Gd2Co7) | 50 | 58 | 181 | 204 | 534.4 | 1.12 | 0.5 | 3 | 2.5 |
| Fe17Ce2(Zn17Th2) | 233 | 58 | 181 | 204 | 534.4 | 1.12 | 0.5 | 3 | 2.5 |
| Fe2Ce(MgCu2) | 235 | 58 | 181 | 204 | 534.4 | 1.12 | 0.5 | 3 | 2.5 |
| Co2Dy(MgCu2) | 141 | 66 | 178 | 192 | 573.0 | 1.22 | 2.5 | 5 | 7.5 |
| Co3Dy(PuNi3) | 450 | 66 | 178 | 192 | 573.0 | 1.22 | 2.5 | 5 | 7.5 |
| Co5Dy(CaCu5) | 977 | 66 | 178 | 192 | 573.0 | 1.22 | 2.5 | 5 | 7.5 |
| Mn23Dy6(Th6Mn23) | 443 | 66 | 178 | 192 | 573.0 | 1.22 | 2.5 | 5 | 7.5 |
| Mn2Dy(MgZn2) | 37 | 66 | 178 | 192 | 573.0 | 1.22 | 2.5 | 5 | 7.5 |
| Ni17Dy2(Th2Ni17) | 170 | 66 | 178 | 192 | 573.0 | 1.22 | 2.5 | 5 | 7.5 |
| Ni2Dy(MgCu2) | 28 | 66 | 178 | 192 | 573.0 | 1.22 | 2.5 | 5 | 7.5 |
| Ni5Dy(CaCu5) | 13 | 66 | 178 | 192 | 573.0 | 1.22 | 2.5 | 5 | 7.5 |
| NiDy(FeB-b) | 64 | 66 | 178 | 192 | 573.0 | 1.22 | 2.5 | 5 | 7.5 |
| Co2Er(TbFe2) | 39 | 68 | 176 | 189 | 589.3 | 1.24 | 1.5 | 6 | 7.5 |
| Co3Er(PuNi3) | 401 | 68 | 176 | 189 | 589.3 | 1.24 | 1.5 | 6 | 7.5 |
| Co5Er(CaCu5) | 1066 | 68 | 176 | 189 | 589.3 | 1.24 | 1.5 | 6 | 7.5 |
| Co7Er(Cu5.44Tb0.78) | 1123 | 68 | 176 | 189 | 589.3 | 1.24 | 1.5 | 6 | 7.5 |
| CoEr3(Fe3C) | 7 | 68 | 176 | 189 | 589.3 | 1.24 | 1.5 | 6 | 7.5 |
| Fe17Er2(Th2Ni17) | 299 | 68 | 176 | 189 | 589.3 | 1.24 | 1.5 | 6 | 7.5 |
| Fe23Er6(Th6Mn23) | 498 | 68 | 176 | 189 | 589.3 | 1.24 | 1.5 | 6 | 7.5 |
| Fe2Er(MgCu2) | 587 | 68 | 176 | 189 | 589.3 | 1.24 | 1.5 | 6 | 7.5 |
| Ni3Er(PuNi3) | 66 | 68 | 176 | 189 | 589.3 | 1.24 | 1.5 | 6 | 7.5 |
| Ni5Er(CaCu5) | 11 | 68 | 176 | 189 | 589.3 | 1.24 | 1.5 | 6 | 7.5 |
| Ni7Er2(Gd2Co7) | 74 | 68 | 176 | 189 | 589.3 | 1.24 | 1.5 | 6 | 7.5 |
| NiEr(FeB-b) | 12 | 68 | 176 | 189 | 589.3 | 1.24 | 1.5 | 6 | 7.5 |
| Ni2Eu(MgCu2) | 139 | 63 | 180 | 198 | 547.1 | 1.2 | 3.0 | 3 | 0.0 |
| Co17Gd2(Zn17Th2) | 1209 | 64 | 180 | 196 | 593.4 | 1.2 | 3.5 | 0 | 3.5 |
| Co2Gd(MgCu2) | 405 | 64 | 180 | 196 | 593.4 | 1.2 | 3.5 | 0 | 3.5 |
| Co3Gd(PuNi3) | 631 | 64 | 180 | 196 | 593.4 | 1.2 | 3.5 | 0 | 3.5 |
| Co3Gd4(Ho6Co4.5) | 233 | 64 | 180 | 196 | 593.4 | 1.2 | 3.5 | 0 | 3.5 |
| Co5Gd(CaCu5) | 1002 | 64 | 180 | 196 | 593.4 | 1.2 | 3.5 | 0 | 3.5 |
| CoGd3(Fe3C) | 143 | 64 | 180 | 196 | 593.4 | 1.2 | 3.5 | 0 | 3.5 |
| Fe17Gd2(Zn17Th2) | 479 | 64 | 180 | 196 | 593.4 | 1.2 | 3.5 | 0 | 3.5 |
| Fe23Gd6(Th6Mn23) | 659 | 64 | 180 | 196 | 593.4 | 1.2 | 3.5 | 0 | 3.5 |
| Fe2Gd(MgCu2) | 814 | 64 | 180 | 196 | 593.4 | 1.2 | 3.5 | 0 | 3.5 |
| Fe3Gd(PuNi3) | 725 | 64 | 180 | 196 | 593.4 | 1.2 | 3.5 | 0 | 3.5 |
| Fe5Gd(CaCu5) | 470 | 64 | 180 | 196 | 593.4 | 1.2 | 3.5 | 0 | 3.5 |
| Mn23Gd6(Th6Mn23) | 465 | 64 | 180 | 196 | 593.4 | 1.2 | 3.5 | 0 | 3.5 |
| Mn2Gd(MgCu2) | 135 | 64 | 180 | 196 | 593.4 | 1.2 | 3.5 | 0 | 3.5 |

Table 2: Descriptors from the 1st to the 40th material.

| g_J | $J_{4f}g_J$ | $J_{4f}(g_J - 1)$ | Z_T | r_T | r_T^{cov} | IP_T | χ_T | S_3d | L_3d |
|--------|-------------|-------------------|-------|-------|-------------|--------|----------|--------|--------|
| 0.8571 | 2.14275 | -0.35725 | 27.0 | 125.0 | 150.0 | 760.4 | 1.88 | 1.5 | 3.0 |
| 0.8571 | 2.14275 | -0.35725 | 27.0 | 125.0 | 150.0 | 760.4 | 1.88 | 1.5 | 3.0 |
| 0.8571 | 2.14275 | -0.35725 | 27.0 | 125.0 | 150.0 | 760.4 | 1.88 | 1.5 | 3.0 |
| 0.8571 | 2.14275 | -0.35725 | 26.0 | 126.0 | 152.0 | 762.5 | 1.83 | 2.0 | 2.0 |
| 0.8571 | 2.14275 | -0.35725 | 26.0 | 126.0 | 152.0 | 762.5 | 1.83 | 2.0 | 2.0 |
| 1.3333 | 9.99975 | 2.49975 | 27.0 | 125.0 | 150.0 | 760.4 | 1.88 | 1.5 | 3.0 |
| 1.3333 | 9.99975 | 2.49975 | 27.0 | 125.0 | 150.0 | 760.4 | 1.88 | 1.5 | 3.0 |
| 1.3333 | 9.99975 | 2.49975 | 27.0 | 125.0 | 150.0 | 760.4 | 1.88 | 1.5 | 3.0 |
| 1.3333 | 9.99975 | 2.49975 | 25.0 | 127.0 | 161.0 | 717.3 | 1.55 | 2.5 | 0.0 |
| 1.3333 | 9.99975 | 2.49975 | 25.0 | 127.0 | 161.0 | 717.3 | 1.55 | 2.5 | 0.0 |
| 1.3333 | 9.99975 | 2.49975 | 28.0 | 124.0 | 124.0 | 737.1 | 1.91 | 1.0 | 3.0 |
| 1.3333 | 9.99975 | 2.49975 | 28.0 | 124.0 | 124.0 | 737.1 | 1.91 | 1.0 | 3.0 |
| 1.3333 | 9.99975 | 2.49975 | 28.0 | 124.0 | 124.0 | 737.1 | 1.91 | 1.0 | 3.0 |
| 1.3333 | 9.99975 | 2.49975 | 28.0 | 124.0 | 124.0 | 737.1 | 1.91 | 1.0 | 3.0 |
| 1.2 | 9.0 | 1.5 | 27.0 | 125.0 | 150.0 | 760.4 | 1.88 | 1.5 | 3.0 |
| 1.2 | 9.0 | 1.5 | 27.0 | 125.0 | 150.0 | 760.4 | 1.88 | 1.5 | 3.0 |
| 1.2 | 9.0 | 1.5 | 27.0 | 125.0 | 150.0 | 760.4 | 1.88 | 1.5 | 3.0 |
| 1.2 | 9.0 | 1.5 | 27.0 | 125.0 | 150.0 | 760.4 | 1.88 | 1.5 | 3.0 |
| 1.2 | 9.0 | 1.5 | 27.0 | 125.0 | 150.0 | 760.4 | 1.88 | 1.5 | 3.0 |
| 1.2 | 9.0 | 1.5 | 26.0 | 126.0 | 152.0 | 762.5 | 1.83 | 2.0 | 2.0 |
| 1.2 | 9.0 | 1.5 | 26.0 | 126.0 | 152.0 | 762.5 | 1.83 | 2.0 | 2.0 |
| 1.2 | 9.0 | 1.5 | 26.0 | 126.0 | 152.0 | 762.5 | 1.83 | 2.0 | 2.0 |
| 1.2 | 9.0 | 1.5 | 28.0 | 124.0 | 124.0 | 737.1 | 1.91 | 1.0 | 3.0 |
| 1.2 | 9.0 | 1.5 | 28.0 | 124.0 | 124.0 | 737.1 | 1.91 | 1.0 | 3.0 |
| 1.2 | 9.0 | 1.5 | 28.0 | 124.0 | 124.0 | 737.1 | 1.91 | 1.0 | 3.0 |
| 1.2 | 9.0 | 1.5 | 28.0 | 124.0 | 124.0 | 737.1 | 1.91 | 1.0 | 3.0 |
| 0.0 | 0.0 | 0.0 | 28.0 | 124.0 | 124.0 | 737.1 | 1.91 | 1.0 | 3.0 |
| 2.0 | 7.0 | 3.5 | 27.0 | 125.0 | 150.0 | 760.4 | 1.88 | 1.5 | 3.0 |
| 2.0 | 7.0 | 3.5 | 27.0 | 125.0 | 150.0 | 760.4 | 1.88 | 1.5 | 3.0 |
| 2.0 | 7.0 | 3.5 | 27.0 | 125.0 | 150.0 | 760.4 | 1.88 | 1.5 | 3.0 |
| 2.0 | 7.0 | 3.5 | 27.0 | 125.0 | 150.0 | 760.4 | 1.88 | 1.5 | 3.0 |
| 2.0 | 7.0 | 3.5 | 27.0 | 125.0 | 150.0 | 760.4 | 1.88 | 1.5 | 3.0 |
| 2.0 | 7.0 | 3.5 | 27.0 | 125.0 | 150.0 | 760.4 | 1.88 | 1.5 | 3.0 |
| 2.0 | 7.0 | 3.5 | 26.0 | 126.0 | 152.0 | 762.5 | 1.83 | 2.0 | 2.0 |
| 2.0 | 7.0 | 3.5 | 26.0 | 126.0 | 152.0 | 762.5 | 1.83 | 2.0 | 2.0 |
| 2.0 | 7.0 | 3.5 | 26.0 | 126.0 | 152.0 | 762.5 | 1.83 | 2.0 | 2.0 |
| 2.0 | 7.0 | 3.5 | 26.0 | 126.0 | 152.0 | 762.5 | 1.83 | 2.0 | 2.0 |
| 2.0 | 7.0 | 3.5 | 26.0 | 126.0 | 152.0 | 762.5 | 1.83 | 2.0 | 2.0 |
| 2.0 | 7.0 | 3.5 | 25.0 | 127.0 | 161.0 | 717.3 | 1.55 | 2.5 | 0.0 |
| 2.0 | 7.0 | 3.5 | 25.0 | 127.0 | 161.0 | 717.3 | 1.55 | 2.5 | 0.0 |

Table 3: Descriptors from the 1st to the 40th material. (cont.)

| J_3d | C_T | C_R | d_{T-T} | d_{R-T} | d_{R-R} | N_{T-R} | N_{R-R} |
|--------|---------|---------|-----------|-----------|-----------|-----------|-----------|
| 4.5 | 0.06846 | 0.00805 | 2.37126 | 2.79635 | 4.07441 | 5.76471 | 38.0 |
| 4.5 | 0.05917 | 0.01183 | 2.46168 | 2.84518 | 4.01800 | 8.4 | 58.0 |
| 4.5 | 0.05449 | 0.01557 | 2.45226 | 2.83193 | 3.12910 | 10.0 | 68.5 |
| 4.0 | 0.06572 | 0.00773 | 2.40832 | 2.83201 | 4.13808 | 3.64706 | 38.0 |
| 4.0 | 0.04110 | 0.02055 | 2.58165 | 3.02725 | 3.16186 | 14.0 | 86.0 |
| 4.5 | 0.04294 | 0.02147 | 2.54417 | 2.98330 | 3.11596 | 14.0 | 86.0 |
| 4.5 | 0.05123 | 0.01708 | 2.47726 | 2.87697 | 3.13757 | 10.88889 | 78.0 |
| 4.5 | 0.08345 | 0.01192 | 1.54703 | 1.22008 | 3.98720 | 6.57143 | 58.0 |
| 2.5 | 0.04780 | 0.01247 | 2.53316 | 3.05688 | 3.57105 | 5.47826 | 50.0 |
| 2.5 | 0.03659 | 0.0183 | 2.68347 | 3.14665 | 3.28657 | 14.0 | 86.0 |
| 4.0 | 0.07398 | 0.0087 | 2.25952 | 2.60907 | 4.33000 | 4.35294 | 36.0 |
| 4.0 | 0.04366 | 0.02183 | 2.53003 | 2.96672 | 3.09864 | 14.0 | 86.0 |
| 4.0 | 0.06136 | 0.01227 | 2.43184 | 2.81112 | 3.96900 | 8.4 | 58.0 |
| 4.0 | 0.02502 | 0.02502 | 2.45561 | 2.81558 | 3.55253 | 11.0 | 106.0 |
| 4.5 | 0.04364 | 0.02182 | 2.53038 | 2.96714 | 3.09907 | 14.0 | 86.0 |
| 4.5 | 0.05188 | 0.01729 | 2.46788 | 2.86461 | 3.12373 | 10.88889 | 78.0 |
| 4.5 | 0.06033 | 0.01207 | 2.44450 | 2.82267 | 4.00400 | 8.4 | 58.0 |
| 4.5 | 0.08541 | 0.0122 | 1.56674 | 1.23563 | 4.03800 | 8.28571 | 58.0 |
| 4.5 | 0.01019 | 0.03056 | 4.19439 | 2.68390 | 3.32898 | 16.0 | 132.0 |
| 4.0 | 0.06635 | 0.00781 | 2.32148 | 2.81572 | 4.14550 | 3.64706 | 36.0 |
| 4.0 | 0.05332 | 0.01391 | 2.44254 | 2.94752 | 3.44330 | 8.6087 | 62.0 |
| 4.0 | 0.04162 | 0.02081 | 2.57069 | 3.01440 | 3.14844 | 14.0 | 86.0 |
| 4.0 | 0.05241 | 0.01747 | 2.46367 | 2.85376 | 3.11046 | 10.88889 | 78.0 |
| 4.0 | 0.06173 | 0.01235 | 2.42800 | 2.80361 | 3.96600 | 8.4 | 58.0 |
| 4.0 | 0.05579 | 0.01594 | 2.42823 | 2.81128 | 3.10758 | 10.0 | 68.5 |
| 4.0 | 0.02567 | 0.02567 | 2.43010 | 2.79557 | 3.52136 | 15.0 | 106.0 |
| 4.0 | 0.04056 | 0.02028 | 2.59296 | 3.04052 | 3.17572 | 14.0 | 86.0 |
| 4.5 | 0.06896 | 0.00811 | 2.36486 | 2.79001 | 4.06341 | 5.76471 | 38.0 |
| 4.5 | 0.04149 | 0.02074 | 2.57352 | 3.01771 | 3.15190 | 14.0 | 86.0 |
| 4.5 | 0.05047 | 0.01682 | 2.48879 | 2.89171 | 3.15397 | 10.22222 | 66.0 |
| 4.5 | 0.02116 | 0.02539 | 2.02400 | 2.85960 | 3.40595 | 12.6 | 107.0 |
| 4.5 | 0.05900 | 0.0118 | 2.44924 | 2.86539 | 3.97300 | 8.4 | 58.0 |
| 4.5 | 0.00941 | 0.02822 | 4.28765 | 2.74391 | 3.45177 | 10.0 | 122.0 |
| 4.0 | 0.06518 | 0.00767 | 2.42005 | 2.96247 | 4.17250 | 4.35294 | 36.0 |
| 4.0 | 0.05210 | 0.01359 | 2.46148 | 2.97038 | 3.47000 | 8.6087 | 62.0 |
| 4.0 | 0.03942 | 0.01971 | 2.61771 | 3.06954 | 3.20603 | 14.0 | 86.0 |
| 4.0 | 0.04746 | 0.01582 | 2.52733 | 2.95576 | 3.22844 | 10.22222 | 66.0 |
| 4.0 | 0.05992 | 0.01198 | 2.41500 | 2.78860 | 4.13000 | 8.4 | 58.0 |
| 2.5 | 0.04705 | 0.01227 | 2.54660 | 3.07310 | 3.59000 | 5.47826 | 50.0 |
| 2.5 | 0.03451 | 0.01725 | 2.73650 | 3.20883 | 3.35152 | 6.0 | 70.0 |

Table 4: Descriptors from the 1st to the 40th material. (*cont.* 2)

| material | T_C | Z_R | r_R | r_R^{cov} | IP_R | χ_R | S_{4f} | L_{4f} | J_{4f} |
|------------------|-------|-------|-------|-------------|--------|----------|----------|----------|----------|
| Ni17Gd2(Th2Ni17) | 189 | 64 | 180 | 196 | 593.4 | 1.2 | 3.5 | 0 | 3.5 |
| Ni2Gd(MgCu2) | 77 | 64 | 180 | 196 | 593.4 | 1.2 | 3.5 | 0 | 3.5 |
| Ni3Gd(PuNi3) | 113 | 64 | 180 | 196 | 593.4 | 1.2 | 3.5 | 0 | 3.5 |
| Ni5Gd(CaCu5) | 32 | 64 | 180 | 196 | 593.4 | 1.2 | 3.5 | 0 | 3.5 |
| NiGd(Th) | 71 | 64 | 180 | 196 | 593.4 | 1.2 | 3.5 | 0 | 3.5 |
| Co2Ho(MgCu2) | 83 | 67 | 176 | 192 | 581.0 | 1.23 | 2.0 | 6 | 8.0 |
| Co5Ho(CaCu5) | 1026 | 67 | 176 | 192 | 581.0 | 1.23 | 2.0 | 6 | 8.0 |
| CoHo3(Fe3C) | 10 | 67 | 176 | 192 | 581.0 | 1.23 | 2.0 | 6 | 8.0 |
| Fe17Ho2(Th2Ni17) | 335 | 67 | 176 | 192 | 581.0 | 1.23 | 2.0 | 6 | 8.0 |
| Fe23Ho6(Th6Mn23) | 507 | 67 | 176 | 192 | 581.0 | 1.23 | 2.0 | 6 | 8.0 |
| Fe2Ho(MgCu2) | 560 | 67 | 176 | 192 | 581.0 | 1.23 | 2.0 | 6 | 8.0 |
| Mn2Ho(MgCu2) | 25 | 67 | 176 | 192 | 581.0 | 1.23 | 2.0 | 6 | 8.0 |
| Ni2Ho(MgCu2) | 16 | 67 | 176 | 192 | 581.0 | 1.23 | 2.0 | 6 | 8.0 |
| Ni5Ho(CaCu5) | 14 | 67 | 176 | 192 | 581.0 | 1.23 | 2.0 | 6 | 8.0 |
| NiHo(FeB-b) | 38 | 67 | 176 | 192 | 581.0 | 1.23 | 2.0 | 6 | 8.0 |
| Co13La(NaZn13) | 1298 | 57 | 187 | 207 | 538.1 | 1.1 | 0.0 | 0 | 0.0 |
| Co5La(CaCu5) | 838 | 57 | 187 | 207 | 538.1 | 1.1 | 0.0 | 0 | 0.0 |
| Fe2Lu(MgCu2) | 580 | 71 | 174 | 187 | 523.5 | 1.27 | 0.0 | 0 | 0.0 |
| Co2Nd(MgCu2) | 108 | 60 | 181 | 201 | 533.1 | 1.14 | 1.5 | 6 | 4.5 |
| Co3Nd(PuNi3) | 381 | 60 | 181 | 201 | 533.1 | 1.14 | 1.5 | 6 | 4.5 |
| Co5Nd(CaCu5) | 910 | 60 | 181 | 201 | 533.1 | 1.14 | 1.5 | 6 | 4.5 |
| CoNd3(Fe3C) | 27 | 60 | 181 | 201 | 533.1 | 1.14 | 1.5 | 6 | 4.5 |
| Fe17Nd2(Zn17Th2) | 327 | 60 | 181 | 201 | 533.1 | 1.14 | 1.5 | 6 | 4.5 |
| Fe17Nd5(Nd5Fe17) | 303 | 60 | 181 | 201 | 533.1 | 1.14 | 1.5 | 6 | 4.5 |
| Fe2Nd(MgCu2) | 453 | 60 | 181 | 201 | 533.1 | 1.14 | 1.5 | 6 | 4.5 |
| Mn23Nd6(Th6Mn23) | 438 | 60 | 181 | 201 | 533.1 | 1.14 | 1.5 | 6 | 4.5 |
| Ni2Nd(MgCu2) | 9 | 60 | 181 | 201 | 533.1 | 1.14 | 1.5 | 6 | 4.5 |
| Ni5Nd(CaCu5) | 7 | 60 | 181 | 201 | 533.1 | 1.14 | 1.5 | 6 | 4.5 |
| Co2Pr(MgCu2) | 45 | 59 | 182 | 203 | 527.0 | 1.13 | 1.0 | 5 | 4.0 |
| Co5Pr(CaCu5) | 931 | 59 | 182 | 203 | 527.0 | 1.13 | 1.0 | 5 | 4.0 |
| CoPr3(Fe3C) | 14 | 59 | 182 | 203 | 527.0 | 1.13 | 1.0 | 5 | 4.0 |
| Fe17Pr2(Zn17Th2) | 280 | 59 | 182 | 203 | 527.0 | 1.13 | 1.0 | 5 | 4.0 |
| Mn23Pr6(Th6Mn23) | 448 | 59 | 182 | 203 | 527.0 | 1.13 | 1.0 | 5 | 4.0 |
| Ni5Pr(CaCu5) | 370 | 59 | 182 | 203 | 527.0 | 1.13 | 1.0 | 5 | 4.0 |
| Co17Sm2(Zn17Th2) | 1193 | 62 | 180 | 198 | 544.5 | 1.17 | 2.5 | 5 | 2.5 |
| Co2Sm(MgCu2) | 230 | 62 | 180 | 198 | 544.5 | 1.17 | 2.5 | 5 | 2.5 |
| Co5Sm(CaCu5) | 1273 | 62 | 180 | 198 | 544.5 | 1.17 | 2.5 | 5 | 2.5 |
| CoSm3(Fe3C) | 78 | 62 | 180 | 198 | 544.5 | 1.17 | 2.5 | 5 | 2.5 |
| Fe17Sm2(Zn17Th2) | 395 | 62 | 180 | 198 | 544.5 | 1.17 | 2.5 | 5 | 2.5 |
| Fe2Sm(MgCu2) | 676 | 62 | 180 | 198 | 544.5 | 1.17 | 2.5 | 5 | 2.5 |

Table 5: Descriptors from the 41st to the 80th material.

| g_J | $J_{4f}g_J$ | $J_{4f}(g_J - 1)$ | Z_T | r_T | r_T^{cov} | IP_T | χ_T | S_3d | L_3d |
|--------|-------------|-------------------|-------|-------|-------------|--------|----------|--------|--------|
| 2.0 | 7.0 | 3.5 | 28.0 | 124.0 | 124.0 | 737.1 | 1.91 | 1.0 | 3.0 |
| 2.0 | 7.0 | 3.5 | 28.0 | 124.0 | 124.0 | 737.1 | 1.91 | 1.0 | 3.0 |
| 2.0 | 7.0 | 3.5 | 28.0 | 124.0 | 124.0 | 737.1 | 1.91 | 1.0 | 3.0 |
| 2.0 | 7.0 | 3.5 | 28.0 | 124.0 | 124.0 | 737.1 | 1.91 | 1.0 | 3.0 |
| 2.0 | 7.0 | 3.5 | 28.0 | 124.0 | 124.0 | 737.1 | 1.91 | 1.0 | 3.0 |
| 1.25 | 10.0 | 2.0 | 27.0 | 125.0 | 150.0 | 760.4 | 1.88 | 1.5 | 3.0 |
| 1.25 | 10.0 | 2.0 | 27.0 | 125.0 | 150.0 | 760.4 | 1.88 | 1.5 | 3.0 |
| 1.25 | 10.0 | 2.0 | 27.0 | 125.0 | 150.0 | 760.4 | 1.88 | 1.5 | 3.0 |
| 1.25 | 10.0 | 2.0 | 26.0 | 126.0 | 152.0 | 762.5 | 1.83 | 2.0 | 2.0 |
| 1.25 | 10.0 | 2.0 | 26.0 | 126.0 | 152.0 | 762.5 | 1.83 | 2.0 | 2.0 |
| 1.25 | 10.0 | 2.0 | 26.0 | 126.0 | 152.0 | 762.5 | 1.83 | 2.0 | 2.0 |
| 1.25 | 10.0 | 2.0 | 25.0 | 127.0 | 161.0 | 717.3 | 1.55 | 2.5 | 0.0 |
| 1.25 | 10.0 | 2.0 | 28.0 | 124.0 | 124.0 | 737.1 | 1.91 | 1.0 | 3.0 |
| 1.25 | 10.0 | 2.0 | 28.0 | 124.0 | 124.0 | 737.1 | 1.91 | 1.0 | 3.0 |
| 1.25 | 10.0 | 2.0 | 28.0 | 124.0 | 124.0 | 737.1 | 1.91 | 1.0 | 3.0 |
| 0.0 | 0.0 | 0.0 | 27.0 | 125.0 | 150.0 | 760.4 | 1.88 | 1.5 | 3.0 |
| 0.0 | 0.0 | 0.0 | 27.0 | 125.0 | 150.0 | 760.4 | 1.88 | 1.5 | 3.0 |
| 0.0 | 0.0 | 0.0 | 26.0 | 126.0 | 152.0 | 762.5 | 1.83 | 2.0 | 2.0 |
| 0.7273 | 3.27285 | -1.22715 | 27.0 | 125.0 | 150.0 | 760.4 | 1.88 | 1.5 | 3.0 |
| 0.7273 | 3.27285 | -1.22715 | 27.0 | 125.0 | 150.0 | 760.4 | 1.88 | 1.5 | 3.0 |
| 0.7273 | 3.27285 | -1.22715 | 27.0 | 125.0 | 150.0 | 760.4 | 1.88 | 1.5 | 3.0 |
| 0.7273 | 3.27285 | -1.22715 | 27.0 | 125.0 | 150.0 | 760.4 | 1.88 | 1.5 | 3.0 |
| 0.7273 | 3.27285 | -1.22715 | 26.0 | 126.0 | 152.0 | 762.5 | 1.83 | 2.0 | 2.0 |
| 0.7273 | 3.27285 | -1.22715 | 26.0 | 126.0 | 152.0 | 762.5 | 1.83 | 2.0 | 2.0 |
| 0.7273 | 3.27285 | -1.22715 | 26.0 | 126.0 | 152.0 | 762.5 | 1.83 | 2.0 | 2.0 |
| 0.7273 | 3.27285 | -1.22715 | 25.0 | 127.0 | 161.0 | 717.3 | 1.55 | 2.5 | 0.0 |
| 0.7273 | 3.27285 | -1.22715 | 28.0 | 124.0 | 124.0 | 737.1 | 1.91 | 1.0 | 3.0 |
| 0.7273 | 3.27285 | -1.22715 | 28.0 | 124.0 | 124.0 | 737.1 | 1.91 | 1.0 | 3.0 |
| 0.8 | 3.2 | -0.8 | 27.0 | 125.0 | 150.0 | 760.4 | 1.88 | 1.5 | 3.0 |
| 0.8 | 3.2 | -0.8 | 27.0 | 125.0 | 150.0 | 760.4 | 1.88 | 1.5 | 3.0 |
| 0.8 | 3.2 | -0.8 | 27.0 | 125.0 | 150.0 | 760.4 | 1.88 | 1.5 | 3.0 |
| 0.8 | 3.2 | -0.8 | 26.0 | 126.0 | 152.0 | 762.5 | 1.83 | 2.0 | 2.0 |
| 0.8 | 3.2 | -0.8 | 25.0 | 127.0 | 161.0 | 717.3 | 1.55 | 2.5 | 0.0 |
| 0.8 | 3.2 | -0.8 | 28.0 | 124.0 | 124.0 | 737.1 | 1.91 | 1.0 | 3.0 |
| 0.2857 | 0.71425 | -1.78575 | 27.0 | 125.0 | 150.0 | 760.4 | 1.88 | 1.5 | 3.0 |
| 0.2857 | 0.71425 | -1.78575 | 27.0 | 125.0 | 150.0 | 760.4 | 1.88 | 1.5 | 3.0 |
| 0.2857 | 0.71425 | -1.78575 | 27.0 | 125.0 | 150.0 | 760.4 | 1.88 | 1.5 | 3.0 |
| 0.2857 | 0.71425 | -1.78575 | 27.0 | 125.0 | 150.0 | 760.4 | 1.88 | 1.5 | 3.0 |
| 0.2857 | 0.71425 | -1.78575 | 26.0 | 126.0 | 152.0 | 762.5 | 1.83 | 2.0 | 2.0 |
| 0.2857 | 0.71425 | -1.78575 | 26.0 | 126.0 | 152.0 | 762.5 | 1.83 | 2.0 | 2.0 |

Table 6: Descriptors from the 41st to the 80th material. (cont.)

| J_3d | C_T | C_R | d_{T-T} | d_{R-T} | d_{R-R} | N_{T-R} | N_{R-R} |
|--------|---------|---------|-----------|-----------|-----------|-----------|-----------|
| 4.0 | 0.06915 | 0.00814 | 2.36257 | 2.72806 | 4.23700 | 4.35294 | 36.0 |
| 4.0 | 0.04265 | 0.02133 | 2.54983 | 2.98994 | 3.12289 | 14.0 | 86.0 |
| 4.0 | 0.05057 | 0.01686 | 2.49359 | 2.88764 | 3.14721 | 10.22222 | 66.0 |
| 4.0 | 0.06042 | 0.01208 | 2.43690 | 2.83421 | 3.96500 | 8.4 | 58.0 |
| 4.0 | 0.02420 | 0.0242 | 2.58495 | 2.89772 | 3.58845 | 11.0 | 92.0 |
| 4.5 | 0.04333 | 0.02167 | 2.53639 | 2.97418 | 3.10643 | 14.0 | 86.0 |
| 4.5 | 0.05994 | 0.01199 | 2.44444 | 2.84056 | 3.97900 | 8.4 | 58.0 |
| 4.5 | 0.01001 | 0.03003 | 4.20705 | 2.69174 | 3.36592 | 14.0 | 131.33333 |
| 4.0 | 0.06652 | 0.00783 | 2.32484 | 2.81005 | 4.15150 | 3.64706 | 36.0 |
| 4.0 | 0.05259 | 0.01372 | 2.45374 | 2.96104 | 3.45909 | 8.6087 | 62.0 |
| 4.0 | 0.04058 | 0.02029 | 2.59261 | 3.04010 | 3.17528 | 14.0 | 86.0 |
| 2.5 | 0.03852 | 0.01926 | 2.63800 | 3.09333 | 3.23088 | 14.0 | 86.0 |
| 4.0 | 0.04410 | 0.02205 | 2.52154 | 2.95677 | 3.08825 | 14.0 | 86.0 |
| 4.0 | 0.06135 | 0.01227 | 2.43006 | 2.81343 | 3.96300 | 8.4 | 58.0 |
| 4.0 | 0.02533 | 0.02533 | 2.44355 | 2.80573 | 3.53764 | 11.0 | 106.0 |
| 4.5 | 0.07100 | 0.00546 | 2.37741 | 3.29960 | 5.67850 | 2.46154 | 26.0 |
| 4.5 | 0.05567 | 0.01113 | 2.47327 | 2.95084 | 3.97000 | 8.4 | 52.0 |
| 4.0 | 0.04234 | 0.02117 | 2.55619 | 2.99740 | 3.13068 | 14.0 | 86.0 |
| 4.5 | 0.04096 | 0.02048 | 2.58448 | 3.03057 | 3.16532 | 14.0 | 86.0 |
| 4.5 | 0.04914 | 0.01638 | 2.51634 | 2.91590 | 3.17848 | 10.22222 | 66.0 |
| 4.5 | 0.05728 | 0.01146 | 2.46505 | 2.90407 | 3.98400 | 8.4 | 52.0 |
| 4.5 | 0.00897 | 0.02692 | 4.33408 | 2.77265 | 3.53652 | 10.0 | 115.33333 |
| 4.0 | 0.06421 | 0.00755 | 2.39377 | 3.07380 | 3.91324 | 4.35294 | 38.0 |
| 4.0 | 0.04675 | 0.01375 | 2.33911 | 2.96841 | 3.25413 | 7.52941 | 56.2 |
| 4.0 | 0.03854 | 0.01927 | 2.63751 | 3.09275 | 3.23027 | 14.0 | 86.0 |
| 2.5 | 0.04510 | 0.01177 | 2.58265 | 3.11660 | 3.64082 | 5.47826 | 50.0 |
| 4.0 | 0.04167 | 0.02083 | 2.56973 | 3.01328 | 3.14727 | 14.0 | 86.0 |
| 4.0 | 0.05919 | 0.01184 | 2.44789 | 2.86077 | 3.97300 | 8.4 | 58.0 |
| 4.5 | 0.04093 | 0.02046 | 2.58518 | 3.03140 | 3.16619 | 14.0 | 86.0 |
| 4.5 | 0.05774 | 0.01155 | 2.46101 | 2.89310 | 3.98200 | 8.4 | 52.0 |
| 4.5 | 0.00890 | 0.0267 | 4.33876 | 2.77540 | 3.55680 | 10.0 | 115.33333 |
| 4.0 | 0.06417 | 0.00755 | 2.41782 | 2.86035 | 4.15442 | 3.64706 | 38.0 |
| 2.5 | 0.04465 | 0.01165 | 2.59140 | 3.12717 | 3.65316 | 5.47826 | 50.0 |
| 4.0 | 0.05914 | 0.01183 | 2.44823 | 2.86193 | 3.97300 | 8.4 | 58.0 |
| 4.5 | 0.06835 | 0.00804 | 2.36874 | 2.80001 | 4.07008 | 5.76471 | 38.0 |
| 4.5 | 0.04180 | 0.0209 | 2.56715 | 3.01025 | 3.14411 | 14.0 | 86.0 |
| 4.5 | 0.05852 | 0.0117 | 2.45327 | 2.87636 | 3.97500 | 8.4 | 58.0 |
| 4.5 | 0.00931 | 0.02793 | 4.29245 | 2.74634 | 3.47712 | 10.0 | 118.0 |
| 4.0 | 0.06473 | 0.00762 | 2.41937 | 2.84701 | 4.15708 | 3.64706 | 38.0 |
| 4.0 | 0.03891 | 0.01946 | 2.62902 | 3.08280 | 3.21988 | 14.0 | 86.0 |

Table 7: Descriptors from the 41st to the 80th material. (*cont.* 2)

| material | T_C | Z_R | r_R | r_R^{cov} | IP_R | χ_R | S_{4f} | L_{4f} | J_{4f} |
|------------------|-------|-------|-------|-------------|--------|----------|----------|----------|----------|
| Fe3Sm(PuNi3) | 657 | 62 | 180 | 198 | 544.5 | 1.17 | 2.5 | 5 | 2.5 |
| Mn23Sm6(Th6Mn23) | 450 | 62 | 180 | 198 | 544.5 | 1.17 | 2.5 | 5 | 2.5 |
| Ni2Sm(MgCu2) | 22 | 62 | 180 | 198 | 544.5 | 1.17 | 2.5 | 5 | 2.5 |
| Co2Tb(TbFe2) | 230 | 65 | 177 | 194 | 565.8 | 1.2 | 3.0 | 3 | 6.0 |
| Co5Tb(CaCu5) | 979 | 65 | 177 | 194 | 565.8 | 1.2 | 3.0 | 3 | 6.0 |
| CoTb3(Fe3C) | 77 | 65 | 177 | 194 | 565.8 | 1.2 | 3.0 | 3 | 6.0 |
| Fe17Tb2(Zn17Th2) | 411 | 65 | 177 | 194 | 565.8 | 1.2 | 3.0 | 3 | 6.0 |
| Fe2Tb(MgCu2) | 701 | 65 | 177 | 194 | 565.8 | 1.2 | 3.0 | 3 | 6.0 |
| Fe3Tb(PuNi3) | 651 | 65 | 177 | 194 | 565.8 | 1.2 | 3.0 | 3 | 6.0 |
| Mn23Tb6(Th6Mn23) | 454 | 65 | 177 | 194 | 565.8 | 1.2 | 3.0 | 3 | 6.0 |
| Mn2Tb(MgCu2) | 48 | 65 | 177 | 194 | 565.8 | 1.2 | 3.0 | 3 | 6.0 |
| Ni2Tb(MgCu2) | 40 | 65 | 177 | 194 | 565.8 | 1.2 | 3.0 | 3 | 6.0 |
| Ni5Tb(CaCu5) | 23 | 65 | 177 | 194 | 565.8 | 1.2 | 3.0 | 3 | 6.0 |
| Co2Tm(MgCu2) | 4 | 69 | 176 | 190 | 596.7 | 1.25 | 1.0 | 5 | 6.0 |
| Co3Tm(PuNi3) | 370 | 69 | 176 | 190 | 596.7 | 1.25 | 1.0 | 5 | 6.0 |
| Co7Tm2(Gd2Co7) | 640 | 69 | 176 | 190 | 596.7 | 1.25 | 1.0 | 5 | 6.0 |
| Fe17Tm2(Th2Ni17) | 271 | 69 | 176 | 190 | 596.7 | 1.25 | 1.0 | 5 | 6.0 |
| Fe2Tm(MgCu2) | 562 | 69 | 176 | 190 | 596.7 | 1.25 | 1.0 | 5 | 6.0 |
| NiTm(FeB-b) | 7 | 69 | 176 | 190 | 596.7 | 1.25 | 1.0 | 5 | 6.0 |
| Mn23Yb6(Th6Mn23) | 406 | 70 | 176 | 187 | 603.4 | 1.1 | 0.5 | 3 | 3.5 |

Table 8: Descriptors from the 81st to the 101st material.

| g_J | $J_{4f}g_J$ | $J_{4f}(g_J - 1)$ | Z_T | r_T | r_T^{cov} | IP_T | χ_T | S_{3d} | L_{3d} |
|--------|-------------|-------------------|-------|-------|-------------|--------|----------|----------|----------|
| 0.2857 | 0.71425 | -1.78575 | 26.0 | 126.0 | 152.0 | 762.5 | 1.83 | 2.0 | 2.0 |
| 0.2857 | 0.71425 | -1.78575 | 25.0 | 127.0 | 161.0 | 717.3 | 1.55 | 2.5 | 0.0 |
| 0.2857 | 0.71425 | -1.78575 | 28.0 | 124.0 | 124.0 | 737.1 | 1.91 | 1.0 | 3.0 |
| 1.5 | 9.0 | 3.0 | 27.0 | 125.0 | 150.0 | 760.4 | 1.88 | 1.5 | 3.0 |
| 1.5 | 9.0 | 3.0 | 27.0 | 125.0 | 150.0 | 760.4 | 1.88 | 1.5 | 3.0 |
| 1.5 | 9.0 | 3.0 | 27.0 | 125.0 | 150.0 | 760.4 | 1.88 | 1.5 | 3.0 |
| 1.5 | 9.0 | 3.0 | 26.0 | 126.0 | 152.0 | 762.5 | 1.83 | 2.0 | 2.0 |
| 1.5 | 9.0 | 3.0 | 26.0 | 126.0 | 152.0 | 762.5 | 1.83 | 2.0 | 2.0 |
| 1.5 | 9.0 | 3.0 | 26.0 | 126.0 | 152.0 | 762.5 | 1.83 | 2.0 | 2.0 |
| 1.5 | 9.0 | 3.0 | 25.0 | 127.0 | 161.0 | 717.3 | 1.55 | 2.5 | 0.0 |
| 1.5 | 9.0 | 3.0 | 25.0 | 127.0 | 161.0 | 717.3 | 1.55 | 2.5 | 0.0 |
| 1.5 | 9.0 | 3.0 | 28.0 | 124.0 | 124.0 | 737.1 | 1.91 | 1.0 | 3.0 |
| 1.5 | 9.0 | 3.0 | 28.0 | 124.0 | 124.0 | 737.1 | 1.91 | 1.0 | 3.0 |
| 1.1667 | 7.0002 | 1.0002 | 27.0 | 125.0 | 150.0 | 760.4 | 1.88 | 1.5 | 3.0 |
| 1.1667 | 7.0002 | 1.0002 | 27.0 | 125.0 | 150.0 | 760.4 | 1.88 | 1.5 | 3.0 |
| 1.1667 | 7.0002 | 1.0002 | 27.0 | 125.0 | 150.0 | 760.4 | 1.88 | 1.5 | 3.0 |
| 1.1667 | 7.0002 | 1.0002 | 26.0 | 126.0 | 152.0 | 762.5 | 1.83 | 2.0 | 2.0 |
| 1.1667 | 7.0002 | 1.0002 | 26.0 | 126.0 | 152.0 | 762.5 | 1.83 | 2.0 | 2.0 |
| 1.1667 | 7.0002 | 1.0002 | 28.0 | 124.0 | 124.0 | 737.1 | 1.91 | 1.0 | 3.0 |
| 1.1429 | 4.00015 | 0.50015 | 25.0 | 127.0 | 161.0 | 717.3 | 1.55 | 2.5 | 0.0 |

Table 9: Descriptors from the 81st to the 101st material. (cont.)

| J_3d | C_T | C_R | d_{T-T} | d_{R-T} | d_{R-R} | N_{T-R} | N_{R-R} |
|--------|---------|---------|-----------|-----------|-----------|-----------|-----------|
| 4.0 | 0.04687 | 0.01562 | 2.53719 | 2.96834 | 3.24242 | 10.22222 | 66.0 |
| 2.5 | 0.04632 | 0.01208 | 2.55984 | 3.08908 | 3.60866 | 5.47826 | 50.0 |
| 4.0 | 0.04234 | 0.02117 | 2.55619 | 2.99740 | 3.13068 | 14.0 | 86.0 |
| 4.5 | 0.04281 | 0.02141 | 2.54665 | 2.98621 | 3.11899 | 14.0 | 86.0 |
| 4.5 | 0.05916 | 0.01183 | 2.45023 | 2.85904 | 3.98000 | 8.4 | 58.0 |
| 4.5 | 0.00968 | 0.02903 | 4.25208 | 2.72082 | 3.41084 | 12.0 | 126.0 |
| 4.0 | 0.06599 | 0.00776 | 2.41336 | 2.82335 | 4.14675 | 3.64706 | 38.0 |
| 4.0 | 0.04038 | 0.02019 | 2.59685 | 3.04508 | 3.18048 | 14.0 | 86.0 |
| 4.0 | 0.04780 | 0.01593 | 2.52128 | 2.94881 | 3.22088 | 10.22222 | 66.0 |
| 2.5 | 0.04729 | 0.01234 | 2.54233 | 3.06794 | 3.58397 | 5.47826 | 50.0 |
| 2.5 | 0.03584 | 0.01792 | 2.70221 | 3.16862 | 3.30952 | 14.0 | 86.0 |
| 4.0 | 0.04332 | 0.02166 | 2.53675 | 2.97460 | 3.10687 | 14.0 | 86.0 |
| 4.0 | 0.06078 | 0.01216 | 2.43479 | 2.82555 | 3.96600 | 8.4 | 58.0 |
| 4.5 | 0.04436 | 0.02218 | 2.51663 | 2.95101 | 3.08223 | 14.0 | 86.0 |
| 4.5 | 0.05218 | 0.01739 | 2.46351 | 2.85910 | 3.11763 | 10.88889 | 78.0 |
| 4.5 | 0.05459 | 0.0156 | 2.43763 | 2.83463 | 3.13565 | 10.0 | 68.5 |
| 4.0 | 0.06686 | 0.00787 | 2.31784 | 2.80705 | 4.13900 | 4.35294 | 36.0 |
| 4.0 | 0.04199 | 0.02099 | 2.56326 | 3.00569 | 3.13934 | 14.0 | 86.0 |
| 4.0 | 0.02598 | 0.02598 | 2.42112 | 2.78329 | 3.50683 | 15.0 | 108.0 |
| 2.5 | 0.05080 | 0.01325 | 2.48225 | 2.99545 | 3.49928 | 8.6087 | 54.0 |

Table 10: Descriptors from the 81st to the 101st material. (cont. 2)

References

- [1] The values of experimental T_C are taken from the AtomWork database, <http://crystdb.nims.go.jp/>.
- [2] Lei Yu, Huan Liu, J. Mach. Learn. Res. **5**, 1205 (2004).
- [3] S. Visalakshi and V. Radha, in 2014 IEEE International Conference on Computational Intelligence and Computing Research (2014), pp. 1-6.
- [4] Hieu Chi Dam, Viet Cuong Nguyen, Tien Lam Pham, Anh Tuan Nguyen, Hiori Kino, Kiyoyuki Terakura, Takashi Miyake, arXiv: 1705.00978v2
- [5] Yusuke Hirayama, private communication.
- [6] Yusuke Hirayama, et al, Scripta Materialia, **138**, 62 (2017).
- [7] Hiroyuki Suzuki, AIP Advances **7**, 56208 (2017).
- [8] Yusuke Harashima, Taro Fukazawa, Hiori Kino and Takashi Miyake, Journal of Applied Physics (accepted).

| material | T_C | Z_R | r_R | r_R^{cov} | IP_R | χ_R | S_{4f} | L_{4f} | J_{4f} |
|------------------|-------|-------|-------|-------------|--------|----------|----------|----------|----------|
| Co17Ce2(Zn17Th2) | 1090 | 58 | 181 | 204 | 534.4 | 1.12 | 0.5 | 3 | 2.5 |
| Co5Ce(CaCu5) | 662 | 58 | 181 | 204 | 534.4 | 1.12 | 0.5 | 3 | 2.5 |
| Co7Ce2(Gd2Co7) | 50 | 58 | 181 | 204 | 534.4 | 1.12 | 0.5 | 3 | 2.5 |
| Fe17Ce2(Zn17Th2) | 233 | 58 | 181 | 204 | 534.4 | 1.12 | 0.5 | 3 | 2.5 |
| Fe2Ce(MgCu2) | 235 | 58 | 181 | 204 | 534.4 | 1.12 | 0.5 | 3 | 2.5 |
| Co2Dy(MgCu2) | 141 | 66 | 178 | 192 | 573.0 | 1.22 | 2.5 | 5 | 7.5 |
| Co3Dy(PuNi3) | 450 | 66 | 178 | 192 | 573.0 | 1.22 | 2.5 | 5 | 7.5 |
| Co5Dy(CaCu5) | 977 | 66 | 178 | 192 | 573.0 | 1.22 | 2.5 | 5 | 7.5 |
| Mn23Dy6(Th6Mn23) | 443 | 66 | 178 | 192 | 573.0 | 1.22 | 2.5 | 5 | 7.5 |
| Mn2Dy(MgZn2) | 37 | 66 | 178 | 192 | 573.0 | 1.22 | 2.5 | 5 | 7.5 |
| Ni17Dy2(Th2Ni17) | 170 | 66 | 178 | 192 | 573.0 | 1.22 | 2.5 | 5 | 7.5 |
| Ni2Dy(MgCu2) | 28 | 66 | 178 | 192 | 573.0 | 1.22 | 2.5 | 5 | 7.5 |
| Ni5Dy(CaCu5) | 13 | 66 | 178 | 192 | 573.0 | 1.22 | 2.5 | 5 | 7.5 |
| NiDy(FeB-b) | 64 | 66 | 178 | 192 | 573.0 | 1.22 | 2.5 | 5 | 7.5 |
| Co2Er(TbFe2) | 39 | 68 | 176 | 189 | 589.3 | 1.24 | 1.5 | 6 | 7.5 |
| Co3Er(PuNi3) | 401 | 68 | 176 | 189 | 589.3 | 1.24 | 1.5 | 6 | 7.5 |
| Co5Er(CaCu5) | 1066 | 68 | 176 | 189 | 589.3 | 1.24 | 1.5 | 6 | 7.5 |
| CoEr3(Fe3C) | 7 | 68 | 176 | 189 | 589.3 | 1.24 | 1.5 | 6 | 7.5 |
| Fe17Er2(Th2Ni17) | 299 | 68 | 176 | 189 | 589.3 | 1.24 | 1.5 | 6 | 7.5 |
| Fe23Er6(Th6Mn23) | 498 | 68 | 176 | 189 | 589.3 | 1.24 | 1.5 | 6 | 7.5 |
| Fe2Er(MgCu2) | 587 | 68 | 176 | 189 | 589.3 | 1.24 | 1.5 | 6 | 7.5 |
| Ni3Er(PuNi3) | 66 | 68 | 176 | 189 | 589.3 | 1.24 | 1.5 | 6 | 7.5 |
| Ni5Er(CaCu5) | 11 | 68 | 176 | 189 | 589.3 | 1.24 | 1.5 | 6 | 7.5 |
| Ni7Er2(Gd2Co7) | 74 | 68 | 176 | 189 | 589.3 | 1.24 | 1.5 | 6 | 7.5 |
| NiEr(FeB-b) | 12 | 68 | 176 | 189 | 589.3 | 1.24 | 1.5 | 6 | 7.5 |
| Ni2Eu(MgCu2) | 139 | 63 | 180 | 198 | 547.1 | 1.2 | 3.0 | 3 | 0.0 |
| Co17Gd2(Zn17Th2) | 1209 | 64 | 180 | 196 | 593.4 | 1.2 | 3.5 | 0 | 3.5 |
| Co2Gd(MgCu2) | 405 | 64 | 180 | 196 | 593.4 | 1.2 | 3.5 | 0 | 3.5 |
| Co3Gd(PuNi3) | 631 | 64 | 180 | 196 | 593.4 | 1.2 | 3.5 | 0 | 3.5 |
| Co3Gd4(Ho6Co4.5) | 233 | 64 | 180 | 196 | 593.4 | 1.2 | 3.5 | 0 | 3.5 |
| Co5Gd(CaCu5) | 1002 | 64 | 180 | 196 | 593.4 | 1.2 | 3.5 | 0 | 3.5 |
| CoGd3(Fe3C) | 143 | 64 | 180 | 196 | 593.4 | 1.2 | 3.5 | 0 | 3.5 |
| Fe17Gd2(Zn17Th2) | 479 | 64 | 180 | 196 | 593.4 | 1.2 | 3.5 | 0 | 3.5 |
| Fe23Gd6(Th6Mn23) | 659 | 64 | 180 | 196 | 593.4 | 1.2 | 3.5 | 0 | 3.5 |
| Fe2Gd(MgCu2) | 814 | 64 | 180 | 196 | 593.4 | 1.2 | 3.5 | 0 | 3.5 |
| Fe3Gd(PuNi3) | 725 | 64 | 180 | 196 | 593.4 | 1.2 | 3.5 | 0 | 3.5 |
| Fe5Gd(CaCu5) | 470 | 64 | 180 | 196 | 593.4 | 1.2 | 3.5 | 0 | 3.5 |
| Mn23Gd6(Th6Mn23) | 465 | 64 | 180 | 196 | 593.4 | 1.2 | 3.5 | 0 | 3.5 |
| Mn2Gd(MgCu2) | 135 | 64 | 180 | 196 | 593.4 | 1.2 | 3.5 | 0 | 3.5 |
| Ni17Gd2(Th2Ni17) | 189 | 64 | 180 | 196 | 593.4 | 1.2 | 3.5 | 0 | 3.5 |

Table 11: Descriptors from the 1st to the 40th material.

| g_J | $J_{4f}g_J$ | $J_{4f}(g_J - 1)$ | Z_T | r_T | r_T^{cov} | IP_T | χ_T | S_3d | L_3d |
|--------|-------------|-------------------|-------|-------|-------------|--------|----------|--------|--------|
| 0.8571 | 2.14275 | -0.35725 | 27.0 | 125.0 | 150.0 | 760.4 | 1.88 | 1.5 | 3.0 |
| 0.8571 | 2.14275 | -0.35725 | 27.0 | 125.0 | 150.0 | 760.4 | 1.88 | 1.5 | 3.0 |
| 0.8571 | 2.14275 | -0.35725 | 27.0 | 125.0 | 150.0 | 760.4 | 1.88 | 1.5 | 3.0 |
| 0.8571 | 2.14275 | -0.35725 | 26.0 | 126.0 | 152.0 | 762.5 | 1.83 | 2.0 | 2.0 |
| 0.8571 | 2.14275 | -0.35725 | 26.0 | 126.0 | 152.0 | 762.5 | 1.83 | 2.0 | 2.0 |
| 1.3333 | 9.99975 | 2.49975 | 27.0 | 125.0 | 150.0 | 760.4 | 1.88 | 1.5 | 3.0 |
| 1.3333 | 9.99975 | 2.49975 | 27.0 | 125.0 | 150.0 | 760.4 | 1.88 | 1.5 | 3.0 |
| 1.3333 | 9.99975 | 2.49975 | 27.0 | 125.0 | 150.0 | 760.4 | 1.88 | 1.5 | 3.0 |
| 1.3333 | 9.99975 | 2.49975 | 25.0 | 127.0 | 161.0 | 717.3 | 1.55 | 2.5 | 0.0 |
| 1.3333 | 9.99975 | 2.49975 | 25.0 | 127.0 | 161.0 | 717.3 | 1.55 | 2.5 | 0.0 |
| 1.3333 | 9.99975 | 2.49975 | 28.0 | 124.0 | 124.0 | 737.1 | 1.91 | 1.0 | 3.0 |
| 1.3333 | 9.99975 | 2.49975 | 28.0 | 124.0 | 124.0 | 737.1 | 1.91 | 1.0 | 3.0 |
| 1.3333 | 9.99975 | 2.49975 | 28.0 | 124.0 | 124.0 | 737.1 | 1.91 | 1.0 | 3.0 |
| 1.3333 | 9.99975 | 2.49975 | 28.0 | 124.0 | 124.0 | 737.1 | 1.91 | 1.0 | 3.0 |
| 1.2 | 9.0 | 1.5 | 27.0 | 125.0 | 150.0 | 760.4 | 1.88 | 1.5 | 3.0 |
| 1.2 | 9.0 | 1.5 | 27.0 | 125.0 | 150.0 | 760.4 | 1.88 | 1.5 | 3.0 |
| 1.2 | 9.0 | 1.5 | 27.0 | 125.0 | 150.0 | 760.4 | 1.88 | 1.5 | 3.0 |
| 1.2 | 9.0 | 1.5 | 27.0 | 125.0 | 150.0 | 760.4 | 1.88 | 1.5 | 3.0 |
| 1.2 | 9.0 | 1.5 | 26.0 | 126.0 | 152.0 | 762.5 | 1.83 | 2.0 | 2.0 |
| 1.2 | 9.0 | 1.5 | 26.0 | 126.0 | 152.0 | 762.5 | 1.83 | 2.0 | 2.0 |
| 1.2 | 9.0 | 1.5 | 26.0 | 126.0 | 152.0 | 762.5 | 1.83 | 2.0 | 2.0 |
| 1.2 | 9.0 | 1.5 | 28.0 | 124.0 | 124.0 | 737.1 | 1.91 | 1.0 | 3.0 |
| 1.2 | 9.0 | 1.5 | 28.0 | 124.0 | 124.0 | 737.1 | 1.91 | 1.0 | 3.0 |
| 1.2 | 9.0 | 1.5 | 28.0 | 124.0 | 124.0 | 737.1 | 1.91 | 1.0 | 3.0 |
| 1.2 | 9.0 | 1.5 | 28.0 | 124.0 | 124.0 | 737.1 | 1.91 | 1.0 | 3.0 |
| 0.0 | 0.0 | 0.0 | 28.0 | 124.0 | 124.0 | 737.1 | 1.91 | 1.0 | 3.0 |
| 2.0 | 7.0 | 3.5 | 27.0 | 125.0 | 150.0 | 760.4 | 1.88 | 1.5 | 3.0 |
| 2.0 | 7.0 | 3.5 | 27.0 | 125.0 | 150.0 | 760.4 | 1.88 | 1.5 | 3.0 |
| 2.0 | 7.0 | 3.5 | 27.0 | 125.0 | 150.0 | 760.4 | 1.88 | 1.5 | 3.0 |
| 2.0 | 7.0 | 3.5 | 27.0 | 125.0 | 150.0 | 760.4 | 1.88 | 1.5 | 3.0 |
| 2.0 | 7.0 | 3.5 | 27.0 | 125.0 | 150.0 | 760.4 | 1.88 | 1.5 | 3.0 |
| 2.0 | 7.0 | 3.5 | 27.0 | 125.0 | 150.0 | 760.4 | 1.88 | 1.5 | 3.0 |
| 2.0 | 7.0 | 3.5 | 27.0 | 125.0 | 150.0 | 760.4 | 1.88 | 1.5 | 3.0 |
| 2.0 | 7.0 | 3.5 | 26.0 | 126.0 | 152.0 | 762.5 | 1.83 | 2.0 | 2.0 |
| 2.0 | 7.0 | 3.5 | 26.0 | 126.0 | 152.0 | 762.5 | 1.83 | 2.0 | 2.0 |
| 2.0 | 7.0 | 3.5 | 26.0 | 126.0 | 152.0 | 762.5 | 1.83 | 2.0 | 2.0 |
| 2.0 | 7.0 | 3.5 | 26.0 | 126.0 | 152.0 | 762.5 | 1.83 | 2.0 | 2.0 |
| 2.0 | 7.0 | 3.5 | 26.0 | 126.0 | 152.0 | 762.5 | 1.83 | 2.0 | 2.0 |
| 2.0 | 7.0 | 3.5 | 25.0 | 127.0 | 161.0 | 717.3 | 1.55 | 2.5 | 0.0 |
| 2.0 | 7.0 | 3.5 | 25.0 | 127.0 | 161.0 | 717.3 | 1.55 | 2.5 | 0.0 |
| 2.0 | 7.0 | 3.5 | 28.0 | 124.0 | 124.0 | 737.1 | 1.91 | 1.0 | 3.0 |

Table 12: Descriptors from the 1st to the 40th material. (cont.)

| J_3d | C_T | C_R | d_{T-T} | d_{R-T} | d_{R-R} | N_{T-R} | N_{R-R} |
|--------|---------|---------|-----------|-----------|-----------|-----------|-----------|
| 4.5 | 0.06846 | 0.00805 | 2.37126 | 2.79635 | 4.07441 | 5.76471 | 38.0 |
| 4.5 | 0.05917 | 0.01183 | 2.46168 | 2.84518 | 4.01800 | 8.4 | 58.0 |
| 4.5 | 0.05449 | 0.01557 | 2.45226 | 2.83193 | 3.12910 | 10.0 | 68.5 |
| 4.0 | 0.06572 | 0.00773 | 2.40832 | 2.83201 | 4.13808 | 3.64706 | 38.0 |
| 4.0 | 0.04110 | 0.02055 | 2.58165 | 3.02725 | 3.16186 | 14.0 | 86.0 |
| 4.5 | 0.04294 | 0.02147 | 2.54417 | 2.98330 | 3.11596 | 14.0 | 86.0 |
| 4.5 | 0.05123 | 0.01708 | 2.47726 | 2.87697 | 3.13757 | 10.88889 | 78.0 |
| 4.5 | 0.08345 | 0.01192 | 1.54703 | 1.22008 | 3.98720 | 6.57143 | 58.0 |
| 2.5 | 0.04780 | 0.01247 | 2.53316 | 3.05688 | 3.57105 | 5.47826 | 50.0 |
| 2.5 | 0.03659 | 0.0183 | 2.68347 | 3.14665 | 3.28657 | 14.0 | 86.0 |
| 4.0 | 0.07398 | 0.0087 | 2.25952 | 2.60907 | 4.33000 | 4.35294 | 36.0 |
| 4.0 | 0.04366 | 0.02183 | 2.53003 | 2.96672 | 3.09864 | 14.0 | 86.0 |
| 4.0 | 0.06136 | 0.01227 | 2.43184 | 2.81112 | 3.96900 | 8.4 | 58.0 |
| 4.0 | 0.02502 | 0.02502 | 2.45561 | 2.81558 | 3.55253 | 11.0 | 106.0 |
| 4.5 | 0.04364 | 0.02182 | 2.53038 | 2.96714 | 3.09907 | 14.0 | 86.0 |
| 4.5 | 0.05188 | 0.01729 | 2.46788 | 2.86461 | 3.12373 | 10.88889 | 78.0 |
| 4.5 | 0.06033 | 0.01207 | 2.44450 | 2.82267 | 4.00400 | 8.4 | 58.0 |
| 4.5 | 0.01019 | 0.03056 | 4.19439 | 2.68390 | 3.32898 | 16.0 | 132.0 |
| 4.0 | 0.06635 | 0.00781 | 2.32148 | 2.81572 | 4.14550 | 3.64706 | 36.0 |
| 4.0 | 0.05332 | 0.01391 | 2.44254 | 2.94752 | 3.44330 | 8.6087 | 62.0 |
| 4.0 | 0.04162 | 0.02081 | 2.57069 | 3.01440 | 3.14844 | 14.0 | 86.0 |
| 4.0 | 0.05241 | 0.01747 | 2.46367 | 2.85376 | 3.11046 | 10.88889 | 78.0 |
| 4.0 | 0.06173 | 0.01235 | 2.42800 | 2.80361 | 3.96600 | 8.4 | 58.0 |
| 4.0 | 0.05579 | 0.01594 | 2.42823 | 2.81128 | 3.10758 | 10.0 | 68.5 |
| 4.0 | 0.02567 | 0.02567 | 2.43010 | 2.79557 | 3.52136 | 15.0 | 106.0 |
| 4.0 | 0.04056 | 0.02028 | 2.59296 | 3.04052 | 3.17572 | 14.0 | 86.0 |
| 4.5 | 0.06896 | 0.00811 | 2.36486 | 2.79001 | 4.06341 | 5.76471 | 38.0 |
| 4.5 | 0.04149 | 0.02074 | 2.57352 | 3.01771 | 3.15190 | 14.0 | 86.0 |
| 4.5 | 0.05047 | 0.01682 | 2.48879 | 2.89171 | 3.15397 | 10.22222 | 66.0 |
| 4.5 | 0.02116 | 0.02539 | 2.02400 | 2.85960 | 3.40595 | 12.6 | 107.0 |
| 4.5 | 0.05900 | 0.0118 | 2.44924 | 2.86539 | 3.97300 | 8.4 | 58.0 |
| 4.5 | 0.00941 | 0.02822 | 4.28765 | 2.74391 | 3.45177 | 10.0 | 122.0 |
| 4.0 | 0.06518 | 0.00767 | 2.42005 | 2.96247 | 4.17250 | 4.35294 | 36.0 |
| 4.0 | 0.05210 | 0.01359 | 2.46148 | 2.97038 | 3.47000 | 8.6087 | 62.0 |
| 4.0 | 0.03942 | 0.01971 | 2.61771 | 3.06954 | 3.20603 | 14.0 | 86.0 |
| 4.0 | 0.04746 | 0.01582 | 2.52733 | 2.95576 | 3.22844 | 10.22222 | 66.0 |
| 4.0 | 0.05992 | 0.01198 | 2.41500 | 2.78860 | 4.13000 | 8.4 | 58.0 |
| 2.5 | 0.04705 | 0.01227 | 2.54660 | 3.07310 | 3.59000 | 5.47826 | 50.0 |
| 2.5 | 0.03451 | 0.01725 | 2.73650 | 3.20883 | 3.35152 | 6.0 | 70.0 |
| 4.0 | 0.06915 | 0.00814 | 2.36257 | 2.72806 | 4.23700 | 4.35294 | 36.0 |

Table 13: Descriptors from the 1st to the 40th material. (*cont.* 2)

| material | T_C | Z_R | r_R | r_R^{cov} | IP_R | χ_R | S_{4f} | L_{4f} | J_{4f} |
|------------------|-------|-------|-------|-------------|--------|----------|----------|----------|----------|
| Ni2Gd(MgCu2) | 77 | 64 | 180 | 196 | 593.4 | 1.2 | 3.5 | 0 | 3.5 |
| Ni3Gd(PuNi3) | 113 | 64 | 180 | 196 | 593.4 | 1.2 | 3.5 | 0 | 3.5 |
| Ni5Gd(CaCu5) | 32 | 64 | 180 | 196 | 593.4 | 1.2 | 3.5 | 0 | 3.5 |
| NiGd(Th) | 71 | 64 | 180 | 196 | 593.4 | 1.2 | 3.5 | 0 | 3.5 |
| Co2Ho(MgCu2) | 83 | 67 | 176 | 192 | 581.0 | 1.23 | 2.0 | 6 | 8.0 |
| Co5Ho(CaCu5) | 1026 | 67 | 176 | 192 | 581.0 | 1.23 | 2.0 | 6 | 8.0 |
| CoHo3(Fe3C) | 10 | 67 | 176 | 192 | 581.0 | 1.23 | 2.0 | 6 | 8.0 |
| Fe17Ho2(Th2Ni17) | 335 | 67 | 176 | 192 | 581.0 | 1.23 | 2.0 | 6 | 8.0 |
| Fe23Ho6(Th6Mn23) | 507 | 67 | 176 | 192 | 581.0 | 1.23 | 2.0 | 6 | 8.0 |
| Fe2Ho(MgCu2) | 560 | 67 | 176 | 192 | 581.0 | 1.23 | 2.0 | 6 | 8.0 |
| Mn2Ho(MgCu2) | 25 | 67 | 176 | 192 | 581.0 | 1.23 | 2.0 | 6 | 8.0 |
| Ni2Ho(MgCu2) | 16 | 67 | 176 | 192 | 581.0 | 1.23 | 2.0 | 6 | 8.0 |
| Ni5Ho(CaCu5) | 14 | 67 | 176 | 192 | 581.0 | 1.23 | 2.0 | 6 | 8.0 |
| NiHo(FeB-b) | 38 | 67 | 176 | 192 | 581.0 | 1.23 | 2.0 | 6 | 8.0 |
| Co13La(NaZn13) | 1298 | 57 | 187 | 207 | 538.1 | 1.1 | 0.0 | 0 | 0.0 |
| Co5La(CaCu5) | 835 | 57 | 187 | 207 | 538.1 | 1.1 | 0.0 | 0 | 0.0 |
| Fe2Lu(MgCu2) | 580 | 71 | 174 | 187 | 523.5 | 1.27 | 0.0 | 0 | 0.0 |
| Co2Nd(MgCu2) | 108 | 60 | 181 | 201 | 533.1 | 1.14 | 1.5 | 6 | 4.5 |
| Co3Nd(PuNi3) | 381 | 60 | 181 | 201 | 533.1 | 1.14 | 1.5 | 6 | 4.5 |
| Co5Nd(CaCu5) | 910 | 60 | 181 | 201 | 533.1 | 1.14 | 1.5 | 6 | 4.5 |
| CoNd3(Fe3C) | 27 | 60 | 181 | 201 | 533.1 | 1.14 | 1.5 | 6 | 4.5 |
| Fe17Nd2(Zn17Th2) | 327 | 60 | 181 | 201 | 533.1 | 1.14 | 1.5 | 6 | 4.5 |
| Fe17Nd5(Nd5Fe17) | 303 | 60 | 181 | 201 | 533.1 | 1.14 | 1.5 | 6 | 4.5 |
| Fe2Nd(MgCu2) | 453 | 60 | 181 | 201 | 533.1 | 1.14 | 1.5 | 6 | 4.5 |
| Mn23Nd6(Th6Mn23) | 438 | 60 | 181 | 201 | 533.1 | 1.14 | 1.5 | 6 | 4.5 |
| Ni2Nd(MgCu2) | 9 | 60 | 181 | 201 | 533.1 | 1.14 | 1.5 | 6 | 4.5 |
| Ni5Nd(CaCu5) | 7 | 60 | 181 | 201 | 533.1 | 1.14 | 1.5 | 6 | 4.5 |
| Co2Pr(MgCu2) | 45 | 59 | 182 | 203 | 527.0 | 1.13 | 1.0 | 5 | 4.0 |
| Co5Pr(CaCu5) | 931 | 59 | 182 | 203 | 527.0 | 1.13 | 1.0 | 5 | 4.0 |
| CoPr3(Fe3C) | 14 | 59 | 182 | 203 | 527.0 | 1.13 | 1.0 | 5 | 4.0 |
| Fe17Pr2(Zn17Th2) | 280 | 59 | 182 | 203 | 527.0 | 1.13 | 1.0 | 5 | 4.0 |
| Mn23Pr6(Th6Mn23) | 448 | 59 | 182 | 203 | 527.0 | 1.13 | 1.0 | 5 | 4.0 |
| Ni5Pr(CaCu5) | 0 | 59 | 182 | 203 | 527.0 | 1.13 | 1.0 | 5 | 4.0 |
| Co17Sm2(Zn17Th2) | 1193 | 62 | 180 | 198 | 544.5 | 1.17 | 2.5 | 5 | 2.5 |
| Co2Sm(MgCu2) | 230 | 62 | 180 | 198 | 544.5 | 1.17 | 2.5 | 5 | 2.5 |
| Co5Sm(CaCu5) | 1016 | 62 | 180 | 198 | 544.5 | 1.17 | 2.5 | 5 | 2.5 |
| CoSm3(Fe3C) | 78 | 62 | 180 | 198 | 544.5 | 1.17 | 2.5 | 5 | 2.5 |
| Fe17Sm2(Zn17Th2) | 395 | 62 | 180 | 198 | 544.5 | 1.17 | 2.5 | 5 | 2.5 |
| Fe2Sm(MgCu2) | 676 | 62 | 180 | 198 | 544.5 | 1.17 | 2.5 | 5 | 2.5 |
| Fe3Sm(PuNi3) | 657 | 62 | 180 | 198 | 544.5 | 1.17 | 2.5 | 5 | 2.5 |

Table 14: Descriptors from the 41st to the 80th material.

| g_J | $J_{4f}g_J$ | $J_{4f}(g_J - 1)$ | Z_T | r_T | r_T^{cov} | IP_T | χ_T | S_3d | L_3d |
|--------|-------------|-------------------|-------|-------|-------------|--------|----------|--------|--------|
| 2.0 | 7.0 | 3.5 | 28.0 | 124.0 | 124.0 | 737.1 | 1.91 | 1.0 | 3.0 |
| 2.0 | 7.0 | 3.5 | 28.0 | 124.0 | 124.0 | 737.1 | 1.91 | 1.0 | 3.0 |
| 2.0 | 7.0 | 3.5 | 28.0 | 124.0 | 124.0 | 737.1 | 1.91 | 1.0 | 3.0 |
| 2.0 | 7.0 | 3.5 | 28.0 | 124.0 | 124.0 | 737.1 | 1.91 | 1.0 | 3.0 |
| 1.25 | 10.0 | 2.0 | 27.0 | 125.0 | 150.0 | 760.4 | 1.88 | 1.5 | 3.0 |
| 1.25 | 10.0 | 2.0 | 27.0 | 125.0 | 150.0 | 760.4 | 1.88 | 1.5 | 3.0 |
| 1.25 | 10.0 | 2.0 | 27.0 | 125.0 | 150.0 | 760.4 | 1.88 | 1.5 | 3.0 |
| 1.25 | 10.0 | 2.0 | 26.0 | 126.0 | 152.0 | 762.5 | 1.83 | 2.0 | 2.0 |
| 1.25 | 10.0 | 2.0 | 26.0 | 126.0 | 152.0 | 762.5 | 1.83 | 2.0 | 2.0 |
| 1.25 | 10.0 | 2.0 | 26.0 | 126.0 | 152.0 | 762.5 | 1.83 | 2.0 | 2.0 |
| 1.25 | 10.0 | 2.0 | 25.0 | 127.0 | 161.0 | 717.3 | 1.55 | 2.5 | 0.0 |
| 1.25 | 10.0 | 2.0 | 28.0 | 124.0 | 124.0 | 737.1 | 1.91 | 1.0 | 3.0 |
| 1.25 | 10.0 | 2.0 | 28.0 | 124.0 | 124.0 | 737.1 | 1.91 | 1.0 | 3.0 |
| 1.25 | 10.0 | 2.0 | 28.0 | 124.0 | 124.0 | 737.1 | 1.91 | 1.0 | 3.0 |
| 0.0 | 0.0 | 0.0 | 27.0 | 125.0 | 150.0 | 760.4 | 1.88 | 1.5 | 3.0 |
| 0.0 | 0.0 | 0.0 | 27.0 | 125.0 | 150.0 | 760.4 | 1.88 | 1.5 | 3.0 |
| 0.0 | 0.0 | 0.0 | 26.0 | 126.0 | 152.0 | 762.5 | 1.83 | 2.0 | 2.0 |
| 0.7273 | 3.27285 | -1.22715 | 27.0 | 125.0 | 150.0 | 760.4 | 1.88 | 1.5 | 3.0 |
| 0.7273 | 3.27285 | -1.22715 | 27.0 | 125.0 | 150.0 | 760.4 | 1.88 | 1.5 | 3.0 |
| 0.7273 | 3.27285 | -1.22715 | 27.0 | 125.0 | 150.0 | 760.4 | 1.88 | 1.5 | 3.0 |
| 0.7273 | 3.27285 | -1.22715 | 27.0 | 125.0 | 150.0 | 760.4 | 1.88 | 1.5 | 3.0 |
| 0.7273 | 3.27285 | -1.22715 | 26.0 | 126.0 | 152.0 | 762.5 | 1.83 | 2.0 | 2.0 |
| 0.7273 | 3.27285 | -1.22715 | 26.0 | 126.0 | 152.0 | 762.5 | 1.83 | 2.0 | 2.0 |
| 0.7273 | 3.27285 | -1.22715 | 26.0 | 126.0 | 152.0 | 762.5 | 1.83 | 2.0 | 2.0 |
| 0.7273 | 3.27285 | -1.22715 | 25.0 | 127.0 | 161.0 | 717.3 | 1.55 | 2.5 | 0.0 |
| 0.7273 | 3.27285 | -1.22715 | 28.0 | 124.0 | 124.0 | 737.1 | 1.91 | 1.0 | 3.0 |
| 0.7273 | 3.27285 | -1.22715 | 28.0 | 124.0 | 124.0 | 737.1 | 1.91 | 1.0 | 3.0 |
| 0.8 | 3.2 | -0.8 | 27.0 | 125.0 | 150.0 | 760.4 | 1.88 | 1.5 | 3.0 |
| 0.8 | 3.2 | -0.8 | 27.0 | 125.0 | 150.0 | 760.4 | 1.88 | 1.5 | 3.0 |
| 0.8 | 3.2 | -0.8 | 27.0 | 125.0 | 150.0 | 760.4 | 1.88 | 1.5 | 3.0 |
| 0.8 | 3.2 | -0.8 | 26.0 | 126.0 | 152.0 | 762.5 | 1.83 | 2.0 | 2.0 |
| 0.8 | 3.2 | -0.8 | 25.0 | 127.0 | 161.0 | 717.3 | 1.55 | 2.5 | 0.0 |
| 0.8 | 3.2 | -0.8 | 28.0 | 124.0 | 124.0 | 737.1 | 1.91 | 1.0 | 3.0 |
| 0.2857 | 0.71425 | -1.78575 | 27.0 | 125.0 | 150.0 | 760.4 | 1.88 | 1.5 | 3.0 |
| 0.2857 | 0.71425 | -1.78575 | 27.0 | 125.0 | 150.0 | 760.4 | 1.88 | 1.5 | 3.0 |
| 0.2857 | 0.71425 | -1.78575 | 27.0 | 125.0 | 150.0 | 760.4 | 1.88 | 1.5 | 3.0 |
| 0.2857 | 0.71425 | -1.78575 | 27.0 | 125.0 | 150.0 | 760.4 | 1.88 | 1.5 | 3.0 |
| 0.2857 | 0.71425 | -1.78575 | 26.0 | 126.0 | 152.0 | 762.5 | 1.83 | 2.0 | 2.0 |
| 0.2857 | 0.71425 | -1.78575 | 26.0 | 126.0 | 152.0 | 762.5 | 1.83 | 2.0 | 2.0 |
| 0.2857 | 0.71425 | -1.78575 | 26.0 | 126.0 | 152.0 | 762.5 | 1.83 | 2.0 | 2.0 |

Table 15: Descriptors from the 41st to the 80th material. (cont.)

| J_3d | C_T | C_R | d_{T-T} | d_{R-T} | d_{R-R} | N_{T-R} | N_{R-R} |
|--------|---------|---------|-----------|-----------|-----------|-----------|-----------|
| 4.0 | 0.04265 | 0.02133 | 2.54983 | 2.98994 | 3.12289 | 14.0 | 86.0 |
| 4.0 | 0.05057 | 0.01686 | 2.49359 | 2.88764 | 3.14721 | 10.22222 | 66.0 |
| 4.0 | 0.06042 | 0.01208 | 2.43690 | 2.83421 | 3.96500 | 8.4 | 58.0 |
| 4.0 | 0.02420 | 0.0242 | 2.58495 | 2.89772 | 3.58845 | 11.0 | 92.0 |
| 4.5 | 0.04333 | 0.02167 | 2.53639 | 2.97418 | 3.10643 | 14.0 | 86.0 |
| 4.5 | 0.05994 | 0.01199 | 2.44444 | 2.84056 | 3.97900 | 8.4 | 58.0 |
| 4.5 | 0.01001 | 0.03003 | 4.20705 | 2.69174 | 3.36592 | 14.0 | 131.33333 |
| 4.0 | 0.06652 | 0.00783 | 2.32484 | 2.81005 | 4.15150 | 3.64706 | 36.0 |
| 4.0 | 0.05259 | 0.01372 | 2.45374 | 2.96104 | 3.45909 | 8.6087 | 62.0 |
| 4.0 | 0.04058 | 0.02029 | 2.59261 | 3.04010 | 3.17528 | 14.0 | 86.0 |
| 2.5 | 0.03852 | 0.01926 | 2.63800 | 3.09333 | 3.23088 | 14.0 | 86.0 |
| 4.0 | 0.04410 | 0.02205 | 2.52154 | 2.95677 | 3.08825 | 14.0 | 86.0 |
| 4.0 | 0.06135 | 0.01227 | 2.43006 | 2.81343 | 3.96300 | 8.4 | 58.0 |
| 4.0 | 0.02533 | 0.02533 | 2.44355 | 2.80573 | 3.53764 | 11.0 | 106.0 |
| 4.5 | 0.07100 | 0.00546 | 2.37741 | 3.29960 | 5.67850 | 2.46154 | 26.0 |
| 4.5 | 0.05567 | 0.01113 | 2.47327 | 2.95084 | 3.97000 | 8.4 | 52.0 |
| 4.0 | 0.04234 | 0.02117 | 2.55619 | 2.99740 | 3.13068 | 14.0 | 86.0 |
| 4.5 | 0.04096 | 0.02048 | 2.58448 | 3.03057 | 3.16532 | 14.0 | 86.0 |
| 4.5 | 0.04914 | 0.01638 | 2.51634 | 2.91590 | 3.17848 | 10.22222 | 66.0 |
| 4.5 | 0.05728 | 0.01146 | 2.46505 | 2.90407 | 3.98400 | 8.4 | 52.0 |
| 4.5 | 0.00897 | 0.02692 | 4.33408 | 2.77265 | 3.53652 | 10.0 | 115.33333 |
| 4.0 | 0.06421 | 0.00755 | 2.39377 | 3.07380 | 3.91324 | 4.35294 | 38.0 |
| 4.0 | 0.04675 | 0.01375 | 2.33911 | 2.96841 | 3.25413 | 7.52941 | 56.2 |
| 4.0 | 0.03854 | 0.01927 | 2.63751 | 3.09275 | 3.23027 | 14.0 | 86.0 |
| 2.5 | 0.04510 | 0.01177 | 2.58265 | 3.11660 | 3.64082 | 5.47826 | 50.0 |
| 4.0 | 0.04167 | 0.02083 | 2.56973 | 3.01328 | 3.14727 | 14.0 | 86.0 |
| 4.0 | 0.05919 | 0.01184 | 2.44789 | 2.86077 | 3.97300 | 8.4 | 58.0 |
| 4.5 | 0.04093 | 0.02046 | 2.58518 | 3.03140 | 3.16619 | 14.0 | 86.0 |
| 4.5 | 0.05774 | 0.01155 | 2.46101 | 2.89310 | 3.98200 | 8.4 | 52.0 |
| 4.5 | 0.00890 | 0.0267 | 4.33876 | 2.77540 | 3.55680 | 10.0 | 115.33333 |
| 4.0 | 0.06417 | 0.00755 | 2.41782 | 2.86035 | 4.15442 | 3.64706 | 38.0 |
| 2.5 | 0.04465 | 0.01165 | 2.59140 | 3.12717 | 3.65316 | 5.47826 | 50.0 |
| 4.0 | 0.05914 | 0.01183 | 2.44823 | 2.86193 | 3.97300 | 8.4 | 58.0 |
| 4.5 | 0.06835 | 0.00804 | 2.36874 | 2.80001 | 4.07008 | 5.76471 | 38.0 |
| 4.5 | 0.04180 | 0.0209 | 2.56715 | 3.01025 | 3.14411 | 14.0 | 86.0 |
| 4.5 | 0.05852 | 0.0117 | 2.45327 | 2.87636 | 3.97500 | 8.4 | 58.0 |
| 4.5 | 0.00931 | 0.02793 | 4.29245 | 2.74634 | 3.47712 | 10.0 | 118.0 |
| 4.0 | 0.06473 | 0.00762 | 2.41937 | 2.84701 | 4.15708 | 3.64706 | 38.0 |
| 4.0 | 0.03891 | 0.01946 | 2.62902 | 3.08280 | 3.21988 | 14.0 | 86.0 |
| 4.0 | 0.04687 | 0.01562 | 2.53719 | 2.96834 | 3.24242 | 10.22222 | 66.0 |

Table 16: Descriptors from the 41st to the 80th material. (*cont.* 2)

| material | T_C | Z_R | r_R | r_R^{cov} | IP_R | χ_R | S_{4f} | L_{4f} | J_{4f} |
|------------------|-------|-------|-------|-------------|--------|----------|----------|----------|----------|
| Mn23Sm6(Th6Mn23) | 450 | 62 | 180 | 198 | 544.5 | 1.17 | 2.5 | 5 | 2.5 |
| Ni2Sm(MgCu2) | 22 | 62 | 180 | 198 | 544.5 | 1.17 | 2.5 | 5 | 2.5 |
| Co2Tb(TbFe2) | 230 | 65 | 177 | 194 | 565.8 | 1.2 | 3.0 | 3 | 6.0 |
| Co5Tb(CaCu5) | 979 | 65 | 177 | 194 | 565.8 | 1.2 | 3.0 | 3 | 6.0 |
| CoTb3(Fe3C) | 77 | 65 | 177 | 194 | 565.8 | 1.2 | 3.0 | 3 | 6.0 |
| Fe17Tb2(Zn17Th2) | 411 | 65 | 177 | 194 | 565.8 | 1.2 | 3.0 | 3 | 6.0 |
| Fe2Tb(MgCu2) | 701 | 65 | 177 | 194 | 565.8 | 1.2 | 3.0 | 3 | 6.0 |
| Fe3Tb(PuNi3) | 651 | 65 | 177 | 194 | 565.8 | 1.2 | 3.0 | 3 | 6.0 |
| Mn23Tb6(Th6Mn23) | 454 | 65 | 177 | 194 | 565.8 | 1.2 | 3.0 | 3 | 6.0 |
| Mn2Tb(MgCu2) | 48 | 65 | 177 | 194 | 565.8 | 1.2 | 3.0 | 3 | 6.0 |
| Ni2Tb(MgCu2) | 40 | 65 | 177 | 194 | 565.8 | 1.2 | 3.0 | 3 | 6.0 |
| Ni5Tb(CaCu5) | 23 | 65 | 177 | 194 | 565.8 | 1.2 | 3.0 | 3 | 6.0 |
| Co2Tm(MgCu2) | 4 | 69 | 176 | 190 | 596.7 | 1.25 | 1.0 | 5 | 6.0 |
| Co3Tm(PuNi3) | 370 | 69 | 176 | 190 | 596.7 | 1.25 | 1.0 | 5 | 6.0 |
| Co7Tm2(Gd2Co7) | 640 | 69 | 176 | 190 | 596.7 | 1.25 | 1.0 | 5 | 6.0 |
| Fe17Tm2(Th2Ni17) | 271 | 69 | 176 | 190 | 596.7 | 1.25 | 1.0 | 5 | 6.0 |
| Fe2Tm(MgCu2) | 562 | 69 | 176 | 190 | 596.7 | 1.25 | 1.0 | 5 | 6.0 |
| NiTm(FeB-b) | 7 | 69 | 176 | 190 | 596.7 | 1.25 | 1.0 | 5 | 6.0 |
| Mn23Yb6(Th6Mn23) | 406 | 70 | 176 | 187 | 603.4 | 1.1 | 0.5 | 3 | 3.5 |

Table 17: Descriptors from the 81st to the 100th material.

| g_J | $J_{4f}g_J$ | $J_{4f}(g_J - 1)$ | Z_T | r_T | r_T^{cov} | IP_T | χ_T | S_{3d} | L_{3d} |
|--------|-------------|-------------------|-------|-------|-------------|--------|----------|----------|----------|
| 0.2857 | 0.71425 | -1.78575 | 25.0 | 127.0 | 161.0 | 717.3 | 1.55 | 2.5 | 0.0 |
| 0.2857 | 0.71425 | -1.78575 | 28.0 | 124.0 | 124.0 | 737.1 | 1.91 | 1.0 | 3.0 |
| 1.5 | 9.0 | 3.0 | 27.0 | 125.0 | 150.0 | 760.4 | 1.88 | 1.5 | 3.0 |
| 1.5 | 9.0 | 3.0 | 27.0 | 125.0 | 150.0 | 760.4 | 1.88 | 1.5 | 3.0 |
| 1.5 | 9.0 | 3.0 | 27.0 | 125.0 | 150.0 | 760.4 | 1.88 | 1.5 | 3.0 |
| 1.5 | 9.0 | 3.0 | 26.0 | 126.0 | 152.0 | 762.5 | 1.83 | 2.0 | 2.0 |
| 1.5 | 9.0 | 3.0 | 26.0 | 126.0 | 152.0 | 762.5 | 1.83 | 2.0 | 2.0 |
| 1.5 | 9.0 | 3.0 | 26.0 | 126.0 | 152.0 | 762.5 | 1.83 | 2.0 | 2.0 |
| 1.5 | 9.0 | 3.0 | 25.0 | 127.0 | 161.0 | 717.3 | 1.55 | 2.5 | 0.0 |
| 1.5 | 9.0 | 3.0 | 25.0 | 127.0 | 161.0 | 717.3 | 1.55 | 2.5 | 0.0 |
| 1.5 | 9.0 | 3.0 | 28.0 | 124.0 | 124.0 | 737.1 | 1.91 | 1.0 | 3.0 |
| 1.5 | 9.0 | 3.0 | 28.0 | 124.0 | 124.0 | 737.1 | 1.91 | 1.0 | 3.0 |
| 1.1667 | 7.0002 | 1.0002 | 27.0 | 125.0 | 150.0 | 760.4 | 1.88 | 1.5 | 3.0 |
| 1.1667 | 7.0002 | 1.0002 | 27.0 | 125.0 | 150.0 | 760.4 | 1.88 | 1.5 | 3.0 |
| 1.1667 | 7.0002 | 1.0002 | 27.0 | 125.0 | 150.0 | 760.4 | 1.88 | 1.5 | 3.0 |
| 1.1667 | 7.0002 | 1.0002 | 26.0 | 126.0 | 152.0 | 762.5 | 1.83 | 2.0 | 2.0 |
| 1.1667 | 7.0002 | 1.0002 | 26.0 | 126.0 | 152.0 | 762.5 | 1.83 | 2.0 | 2.0 |
| 1.1667 | 7.0002 | 1.0002 | 28.0 | 124.0 | 124.0 | 737.1 | 1.91 | 1.0 | 3.0 |
| 1.1429 | 4.00015 | 0.50015 | 25.0 | 127.0 | 161.0 | 717.3 | 1.55 | 2.5 | 0.0 |

Table 18: Descriptors from the 81st to the 100th materials. (cont.)

| J_3d | C_T | C_R | d_{T-T} | d_{R-T} | d_{R-R} | N_{T-R} | N_{R-R} |
|--------|---------|---------|-----------|-----------|-----------|-----------|-----------|
| 2.5 | 0.04632 | 0.01208 | 2.55984 | 3.08908 | 3.60866 | 5.47826 | 50.0 |
| 4.0 | 0.04234 | 0.02117 | 2.55619 | 2.99740 | 3.13068 | 14.0 | 86.0 |
| 4.5 | 0.04281 | 0.02141 | 2.54665 | 2.98621 | 3.11899 | 14.0 | 86.0 |
| 4.5 | 0.05916 | 0.01183 | 2.45023 | 2.85904 | 3.98000 | 8.4 | 58.0 |
| 4.5 | 0.00968 | 0.02903 | 4.25208 | 2.72082 | 3.41084 | 12.0 | 126.0 |
| 4.0 | 0.06599 | 0.00776 | 2.41336 | 2.82335 | 4.14675 | 3.64706 | 38.0 |
| 4.0 | 0.04038 | 0.02019 | 2.59685 | 3.04508 | 3.18048 | 14.0 | 86.0 |
| 4.0 | 0.04780 | 0.01593 | 2.52128 | 2.94881 | 3.22088 | 10.22222 | 66.0 |
| 2.5 | 0.04729 | 0.01234 | 2.54233 | 3.06794 | 3.58397 | 5.47826 | 50.0 |
| 2.5 | 0.03584 | 0.01792 | 2.70221 | 3.16862 | 3.30952 | 14.0 | 86.0 |
| 4.0 | 0.04332 | 0.02166 | 2.53675 | 2.97460 | 3.10687 | 14.0 | 86.0 |
| 4.0 | 0.06078 | 0.01216 | 2.43479 | 2.82555 | 3.96600 | 8.4 | 58.0 |
| 4.5 | 0.04436 | 0.02218 | 2.51663 | 2.95101 | 3.08223 | 14.0 | 86.0 |
| 4.5 | 0.05218 | 0.01739 | 2.46351 | 2.85910 | 3.11763 | 10.88889 | 78.0 |
| 4.5 | 0.05459 | 0.0156 | 2.43763 | 2.83463 | 3.13565 | 10.0 | 68.5 |
| 4.0 | 0.06686 | 0.00787 | 2.31784 | 2.80705 | 4.13900 | 4.35294 | 36.0 |
| 4.0 | 0.04199 | 0.02099 | 2.56326 | 3.00569 | 3.13934 | 14.0 | 86.0 |
| 4.0 | 0.02598 | 0.02598 | 2.42112 | 2.78329 | 3.50683 | 15.0 | 108.0 |
| 2.5 | 0.05080 | 0.01325 | 2.48225 | 2.99545 | 3.49928 | 8.6087 | 54.0 |

Table 19: Descriptors from the 81st to the 100th material. (*cont.* 2)